ÇUKUROVA UNIVERSITY
INSTITUTE OF NATURAL AND APPLIED SCIENCES

MSc THESIS

Ediz ÇARDAK

ENERGY AND EXERGY ANALYSIS OF AN INTER-CITY BUS AIR-CONDITIONING SYSTEM WORKING WITH DIFFERENT REFRIGERANTS

DEPARTMENT OF AUTOMOTIVE ENGINEERING

ADANA-2017

ÇUKUROVA UNIVERSITY
INSTITUTE OF NATURAL AND APPLIED SCIENCES

ENERGY AND EXERGY ANALYSIS OF AN INTER-CITY BUS AIR-CONDITIONING SYSTEM WORKING WITH DIFFERENT REFRIGERANTS

Ediz ÇARDAK

MSc THESIS

DEPARTMENT OF AUTOMOTIVE ENGINEERING

We certify that the thesis titled above was reviewed and approved for the award of degree of the Master of Science by the board of jury on …/…/2017

……………………………...	……………………………….	………………………...
Assoc. Prof. Dr. Mehmet BİLGİLİ	Assoc. Prof. Dr. Abdulkadir YAŞAR	Asst. Prof. Dr. Fırat EKİNCİ
SUPERVISOR	MEMBER	MEMBER

This MSc Thesis is written at the Department of Institute of Natural and Applied Sciences of Çukurova University.
Registration Number:

Prof. Dr. Mustafa GÖK
Director
Institute of Natural and Applied Sciences

ABSTRACT

MSc THESIS

ENERGY AND EXERGY ANALYSIS OF AN INTER-CITY BUS AIR-CONDITIONING SYSTEM WORKING WITH DIFFERENT REFRIGERANTS

Ediz ÇARDAK

ÇUKUROVA UNIVERSITY
INSTITUTE OF NATURAL AND APPLIED SCIENCES
DEPARTMENT OF AUTOMOTIVE ENGINEERING

Supervisor : Assoc. Prof. Dr. Mehmet BİLGİLİ
Year: 2017, Pages: 75
Jury : Assoc. Prof. Dr. Mehmet BİLGİLİ
: Assoc. Prof. Dr. Abdulkadir YAŞAR
: Asst. Prof. Dr. Fırat EKİNCİ

In this thesis, energy and exergy analysis of inter-city bus air conditioning (ICBAC) system are performed using different refrigerants and air mixing ratios (MRs). Adana province of Turkey was chosen as the study region. Firstly, a coach bus, which is used for inter-city passenger transportation in USA, with a passenger capacity of 56 persons was selected. Hourly Analysis Program (HAP) was used to determine the hourly cooling load capacity of the selected inter-city bus model. In cooling load calculation of the inter-city bus, climate data such as dry bulb temperature, wet bulb temperature and solar radiation of the Adana province were used. Commonly used refrigerants R404A, R410A, R502, R507, R22, R290, R134a, R500 and R600a were selected for use in the ICBAC system. Obtained Coefficient of Performance (COP), exergy efficiency and exergy destruction values of ICBAC system and its components for July were evaluated. Results reveals that the performance of the ICBAC system are substantially affected from refrigerants and MRs, and R600a has the minimum total exergy destruction among all studied refrigerants. Minimum total exergy destruction value of R600a was obtained as 3.88 kW for MR=0.05, and maximum total exergy destruction value was calculated as 7.02 kW for MR=0.5.

Keywords: Air-conditioning, Refrigerants, Exergy, Exergy efficiency, Inter-city bus.

ÖZ

YÜKSEK LİSANS TEZİ

ŞEHİRLERARASI BİR OTOBÜSE AİT KLİMANIN FARKLI SOĞUTUCU AKIŞKLANLARA GÖRE ENERJİ VE EKSERJİ ANALİZİ

Ediz ÇARDAK

ÇUKUROVA ÜNİVERSİTESİ
FEN BİLİMLERİ ENSTİTÜSÜ
OTOMOTİV MÜHENDİSLİĞİ ANABİLİM DALI

Danışman : Doç. Dr. Mehmet Bilgili
: Yıl: 2017, Sayfa: 75
Jüri : Doç. Dr. Mehmet BİLGİLİ
: Doç. Dr. Abdulkadir YAŞAR
: Yrd. Doç. Dr. Fırat EKİNCİ

Bu tezde, şehirlerarası bir otobüse ait klimanın (ICBAC) farklı soğutucu akışkanlara ve hava karışım oranlarına (MRs) göre enerji ve ekserji analizi yapılmıştır. Çalışma bölgesi olarak Türkiye'nin Adana ili seçilmiştir. Öncelikle, ABD'de şehirlerarası ulaşımda kullanılan ve 56 yolcu kapasitesine sahip bir otobüs modeli seçilmiştir. Otobüsün soğutma yükünün hesaplanması için Saatlik Analiz Programı (HAP) kullanılmıştır. Adana iline ait kuru ve yaş termometre sıcaklığı, güneş ışınım verileri gibi iklim verileri soğutma yükünün hesaplanmasında kullanılmıştır. Sistemin soğutma etkinliği (COP) ve ekserji verimlilikleri; seçilen R404A, R410A, R502, R507, R22, R290, R134a, R500 ve R600a soğutucu akışkanları için Temmuz ayı verilerine göre hesaplanmış ve sonuçlar üzerinden değerlendirme yapılmıştır. Sonuçlar ICBAC sistemi ve sistem bileşenlerinin performansının farklı soğutucu akışkanlardan ve MR değerlerinden doğrudan etkilendiğini ortaya çıkarmıştır. Ayrıca, soğutucu akışkanlar arasında R600a'nın en düşük toplam ekserji yok oluş değerine sahip olduğu belirlenmiştir. R600a'ya ait en düşük toplam ekserji yok oluş değerinin MR=0.05'de 3.883 kW ve en yüksek toplam ekserji yok oluş değerinin MR=0.5'de 7.02 kW olduğu tespit edilmiştir.

Anahtar Kelimeler: Ekserji, Ekserji verimi, Soğutucu Akışkan, Klima, Şehirlerarası otobüs

GENİŞLETİLMİŞ ÖZET

Sanayi devrimiyle birlikte insan hayatı kolaylaşmıştır. Sanayi devrimden bu yana teknoloji ve endüstrileşme alanında olan gelişmeler hızla artmaktadır. Bu gelişmelere paralel olarak enerjiye olan ihtiyaçta da her geçen gün artmaktadır.

Enerji kullanımının birçok yararı olmasının yanında, CO_2 emisyonu gibi çevreye zarar veren bazı sonuçlara da sebep olmaktadır. Fosil yakıtların enerji kaynağı olarak kullanılması ve buna bağlı olarak CO_2 emisyonunun artması buna örnek olarak verilebilir. Eğer bu konuda önlem alınmazsa, daha ciddi çevresel sorunların ortaya çıkması muhtemeldir.

CO_2 emisyonu ve buna bağlı çevresel kirliliğin önlenmesi için toplu taşıma sektörü de dâhil olmak üzere her sektörün alması gereken bazı önlemler vardır. Bu önlemlerden bir tanesi enerjiyi daha verimli kullanmaktır. Bir sistemde enerjinin verimli kullanılabilmesi, yüksek ekserji verimliliği ve düşük ekserji yok oluş değerlerine ulaşılmasıyla sağlanabilir.

Nüfusun artmasına bağlı olarak toplu taşımaya olan ihtiyaçta her geçen gün artmaktadır. Toplu taşıma sektörü enerji tüketimi konusunda önemli bir paya sahiptir. Şehirlerarası otobüsler ise toplu taşımanın en önemli unsurlarından birisidir.

Şehirlerarası otobüslerde, ikinci en çok enerji tüketimi yapan sistemin klima sistemleri olduğu ve klima sistemlerinin verimsiz bir şekilde çalıştığı yapılan çeşitli bilimsel çalışmalarla belirlenmiştir. Enerjinin verimli kullanılması düşük yakıt tüketimine ve buna bağlı olarak da CO_2 emisyonunun düşmesine katkı sağlayacaktır. Bu tezde, şehirlerarası bir otobüse ait klimanın (ICBAC) farklı soğutucu akışkanlara ve hava karışım oranlarına (MR) göre enerji ve ekserji analizi yapılmıştır.

Tezin hazırlanması sırasında, önceki çalışmalar bölümü genelden özele gitmek üzere 4'e ayrılarak incelenmiştir. Bu bölümler sırasıyla "çeşitli çalışmalarda enerji ve ekserji analizi", "otomotiv klima sistemleri üzerine çalışmalar", "klima sistemlerinde enerji ve ekserji analizi" ve "otomotiv klima sistemlerinde enerji ve ekserji analizi" olarak tanımlanmıştır.

Çalışma bölgesi olarak Türkiye'nin Adana ili seçilmiştir. Öncelikle, ABD'de şehirlerarası ulaşımda kullanılan ve 56 yolcu kapasitesine sahip "Temsa TS 45" otobüs modeli seçilmiştir. Seçilen otobüs, paslanmaz çelik gövdeye ve 6 silindirli klima kompresörü olan yüksek kapasiteli bir iklimlendirme sistemine sahiptir. Otobüsün iklimlendirme sisteminde R134a soğutucu akışkanı kullanılmaktadır.

Şehirlerarası otobüsün soğutma yükünün hesaplanması için Saatlik Analiz Programı (HAP) kullanılmıştır. Soğutma yükünün hesaplanmasında, Adana iline ait kuru ve yaş termometre sıcaklığı, güneş ışınım verileri gibi iklim verileri kullanılmıştır. Yük hesaplamaları ve enerji analizleri American Society of Heating, Refrigerating, and Air-Conditioning Engineers (ASHRAE) onaylı aktarma fonksiyonu metodu ve detaylandırılmış 8760 saatlik enerji simülasyonu tekniği ile yapılmıştır.

R404A, R410A, R502, R507, R22, R290, R134a, R500 ve R600a soğutucu akışkanları, farklı soğutucu akışkan çeşitleri olarak kullanılmak üzere ICBAC sistemi ekserji analizi için seçilmiştir. Seçilen soğutucu akışkanların termodinamik özellikleri CoolPack V2.85 programı kullanılarak hesaplanmıştır. ICBAC sistemi ve onun bileşenlerine ait COP, ekserji verimliliği ve ekserji yok oluş değerleri hesaplanmış ve çıkan sonuçların değerlendirilmeleri tüm soğutucu akışkanların için yapılmıştır.

ICBAC sistemi varsayımları ve analizlerinde, MR değerinin 0.05 ve 0.5 arasında olduğu varsayılmıştır. Maksimum ısı kazancı değeri 25.96 kW olarak, Temmuz ayı içinde ve saat 17:00'de elde edilmiştir. Şehirler arası otobüs kabininin içi 24.4 °C kuru termometre sıcaklığı ve %50 bağıl nemde muhafaza edilirken, dış ortam kuru ve yaş termometre sıcaklığı 36.8 °C ve 25.7 °C olarak alınmıştır.

Soğutma devresi hesaplamalarında, soğutucu akışkanın buharlaşma sıcaklığı soğutma serpantini çiğ noktası sıcaklığına denk kabul edilmiştir. Dış hava ve iç hava karışımı MR = 0.5 olarak karıştırıldığında karışım sıcaklığı 28.53 °C olarak bulunmuştur.

ICBAC sistem parçalarının hesaplamaları sırasında klima soğutma kapasitesi MR=0.5 için 49.03 kW olarak bulunmuştur. Bulunan bu değerin Figür 4.7'de verilen resmi değer olan 48 kW değerine çok yakın olması, ICBAC sistemi ve sistem bileşenleri için yapılan hesaplamaların doğruluğunu ortaya çıkarmaktadır.

Elde edilen sonuçlara göre, toplam ekserji yok oluş değerleri MR'a paralel olarak kayda değer biçimde artarken, genel ekserji verimi daha küçük oranlarda artmaktadır. Ayrıca, R600a soğutucu akışkanı en yüksek genel ekserji verimi ve en düşük toplam ekserji yok oluş değerlerine sahipken, R404A akışkanı en düşük genel ekserji verimi ve en yüksek toplam ekserji yok oluş değerlerine sahiptir. Bu sonuçlar, Temsa TS 45 şehirlerarası otobüsünde kullanılmakta olan R134a soğutucu akışkanının ekserji verimlilik değerlerinin, R600a akışkanından daha düşük olduğunu ortaya koymaktadır.

R600a ve R404A soğutucu akışkanlarının maksimum toplam ekserji yok oluş değerleri, MR=0.5'de sırasıyla 7.02 kW ve 8.37 kW olarak tespit edilirken, minimum toplam ekserji yok oluş değerleri, MR=0.05'de sırasıyla. 3.88 kW ve 4.69 kW olarak tespit edilmiştir. Ayrıca, R600a ve R404A akışkanlarının maksimum genel ekserji verimi değerleri, MR=0.5 değerinde sırasıyla % 46.45 ve %40.00 olarak tespit edilirken, minimum genel ekserji verimi değerleri, MR=0.05 değerinde sırasıyla %45.67 ve %45.67 olarak tespit edilmiştir. Sonuçlar ICBAC sistemi performansının farklı soğutucu akışkanlardan ve MR değerlerinden doğrudan etkilendiğini göstermiştir.

Soğutucu akışkanlar arasında R600a'nın en düşük toplam ekserji yok oluş değerine sahip olduğu hesaplanmıştır. R600a'ya ait en düşük toplam ekserji yok oluş değerinin MR=0.05'de 3.88 kW ve en yüksek toplam yok oluş değerinin MR=0.5'de 7.02 kW olduğu tespit edilmiştir. Bundan sonraki çalışmalarda, R600a soğutucu akışkanının, otomotiv iklimlendirme sistemlerinde R134a akışkanı yerine kullanılmaya başlanması araştırılmalıdır.

ACKNOWLEDGEMENTS

First of all, I would like to express my sincere gratitude to Assoc. Prof. Dr. Mehmet BİLGİLİ for his supervision throughout my studies. His patience, guidance and valuable time spared for the development of this work was very important for during my MSc studies. His approach to the students and solving the problems will certainly help me in my future academic carrier.

I would also like to thank to the TEMSA Company and especially to my colleagues for their support and motivation.

Special thanks to Arif Emre AKTAŞ for his contribution throughout my research activities.

Last but not least, my heartfelt thanks to my mother Serpil ÇARDAK, my father Ahmet ÇARDAK and my brother Emre ÇARDAK for their absolute, continuous and unconditional support. I certainly wouldn't have succeeded to finish my thesis without their support.

TABLE OF CONTENTS **PAGE**

LIST OF TABLES **PAGE**

LIST OF FIGURES **PAGE**

LIST OF ABBREVIATIONS AND NOMENCLATURE

A	: Area
AC	: Air Conditioning
AAC	: Automotive Air Conditioning
BPF	: By-pass factor
ANN	: Artificial Neural Network
ASHRAE	: American Society of Heating, Refrigerating, and Air-Conditioning Engineers
c	: Specific heat
CFBB	: Circulation Fluidized Bed Boiler
CLTD	: Cooling load temperature difference
COP	: Coefficient of Performance
$\dot{E}$	: Energy
$\dot{E}x$	: Exergy rate
FBCC	: Fluidized Bed Coal Combustor
GWP	: Global-Warming Potential
h	: Enthalpy per unit mass
HAP	: Hourly Analysis Program
HVAC	: Heating, Ventilating, and Air Conditioning
ICBAC	: Inter-City Bus Air Conditioning
$\dot{m}$	: Mass flow rate
MLP	: Multilayer Perceptron
MR	: Air Mixing Ratio
NARX	: Nonlinear Autoregressive Exogenous
OEM	: Original Equipment Manufacturer
ORC	: Organic Rankine Cycle
P	: Pressure

$\dot{Q}$	: Heat transfer rate
R22	: Chlorodifluoromethane
R134a	: 1,1,1,2-Tetrafluoroethane
R290	: Propane
R404A	: R-125/143a/134a (44±2/52±1/4±2)
R410A	: R-32/125 (50+.5,–1.5/50+1.5,–.5)
R502	: R-22/115 (48.8/51.2)
R507	: R-125/143a (50/50)
R500	: R-12/152a (73.8/26.2)
R600a	: Isobutane
RBN	: Radial Basis Network
$\dot{S}$	: Entropy
SC	: Shading coefficient
SHGF	: Solar heat gain factor
T	: Temperature
T_{ADP}	: Apparatus Dew Point Temperature
T-ORVC	: Organic Rankine Vapor Compression
U	: Heat transfer coefficient
V	: Velocity of the system
w	: Humidity ratio
$\dot{W}$	: Work
η	: Isentropic efficiency
ψ	: Exergy efficiency of various steady-flow devices

Superscripts and Subscripts

ADP	: Apparatus dew-point
avg	: Average
comp	: Compressor
cond	: Condenser
dest	: Destruction
evap	: Evaporator
exp.val.	: Expansion valve
gen	: Generation
i	: Indoor air
l	: Latent
m	: Mixed
max	: Maximum
o	: Outdoor air
p	: Pressure
ref	: Refrigerant
rev	: Reversible
s	: Sensible
s	: Supplied air
w	: Condensate

1. INTRODUCTION

Our life has become easier with the industrial revolution. Industrialization and technology bring many advantages such as efficient production, cheaper prices and thus improved quality of life. With economic and technological developments, demands for energy consumption also increased at an accelerated rate throughout the years. Despite all the benefits that come with energy consumption, it has some negative effects on environment. For instance, usage of fossil fuel energy sources such as crude oil and coal causes increment in CO_2 concentration (IEA, 2016).

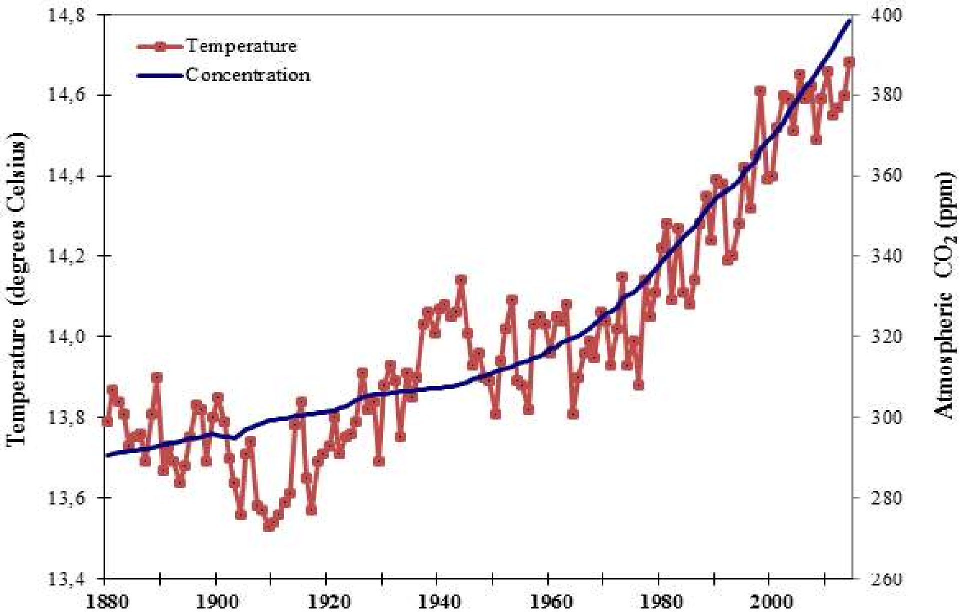

Figure 1.1. Average global temperature and atmospheric CO_2 concentration, 1880-2014 (Earth Policy Institute, 2014)

The average global temperature and atmospheric CO_2 concentration change from 1880 to 2014 are presented in Figure 1.1. As demonstrated in the figure, temperature is distinctly increasing with increasing CO_2 concentration throughout the years, especially for last 30 years. It can be concluded that the energy-related

CO_2 emissions will affect environment perilously, if precautions are not taken. In this regard, an energy revolution is required to decrease CO_2 emissions and thus average global temperature. Almost every sector can contribute to the reduction of CO_2 emissions.

Contribution of technologies and sectors to global cumulative CO_2 reductions is shown in Figure 1.2. As can be observed from the figure, energy efficiency has an important role to reduce CO_2 emissions in many sectors such as transport and buildings. In this section, we will be focused on energy efficiency of transportation and thus fuel consumption in Turkey.

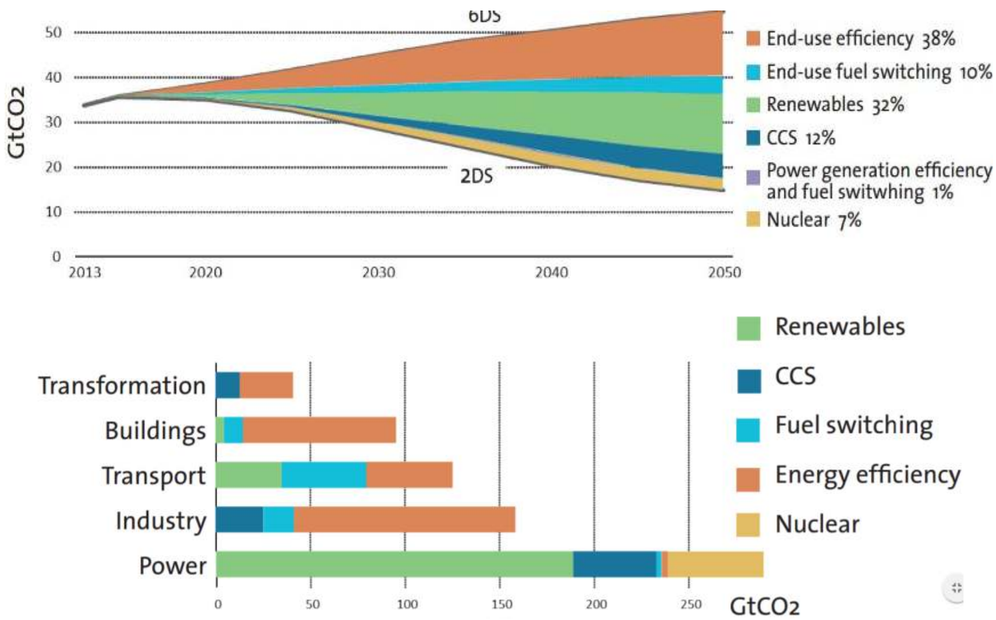

Figure 1.2. Contribution of technologies and sectors to global cumulative CO_2 reductions (IEA, 2016)

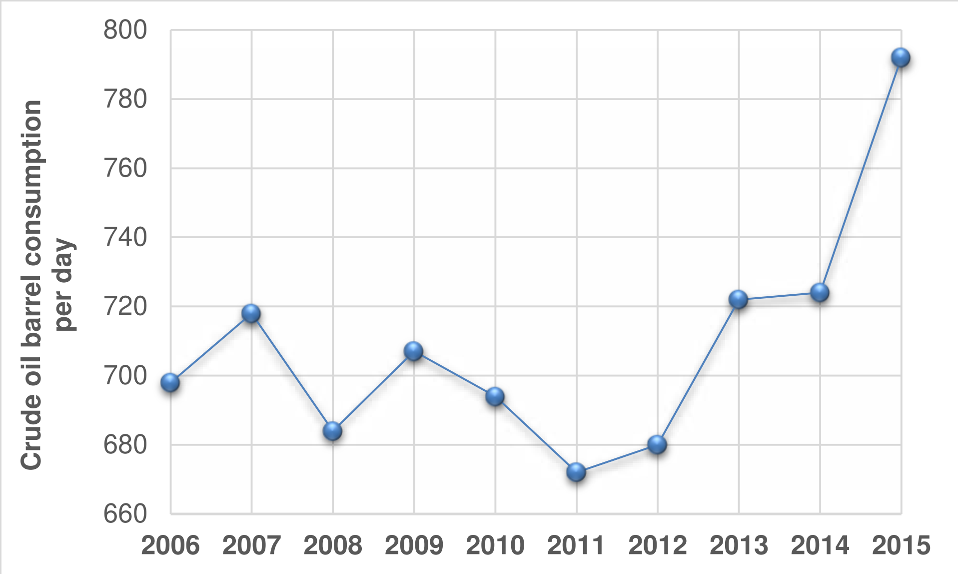

Figure 1.3. Crude oil barrel consumption per day in Turkey, 2006-2015 (Turkish Petroleum, 2015)

Figure 1.3 presents the crude oil barrel consumption per day in Turkey between 2006 and 2015. According to the data, crude oil consumption has an accelerated increment after 2011.

Number of total vehicles in Turkey between 1966 and 2016 is shown in Figure 1.4, while number of total buses is displayed in Figure 1.5. As it is seen in the figures, the number of buses and total vehicles is increasing rapidly in Turkey. With growing numbers of vehicles, energy efficiency becomes more important in public transportation. It is worthwhile to mention that buses are one of the most important figures of public transportation and they are designed to carry many passengers. In this regard, energy efficiency of inter-city buses will be main focus of the study.

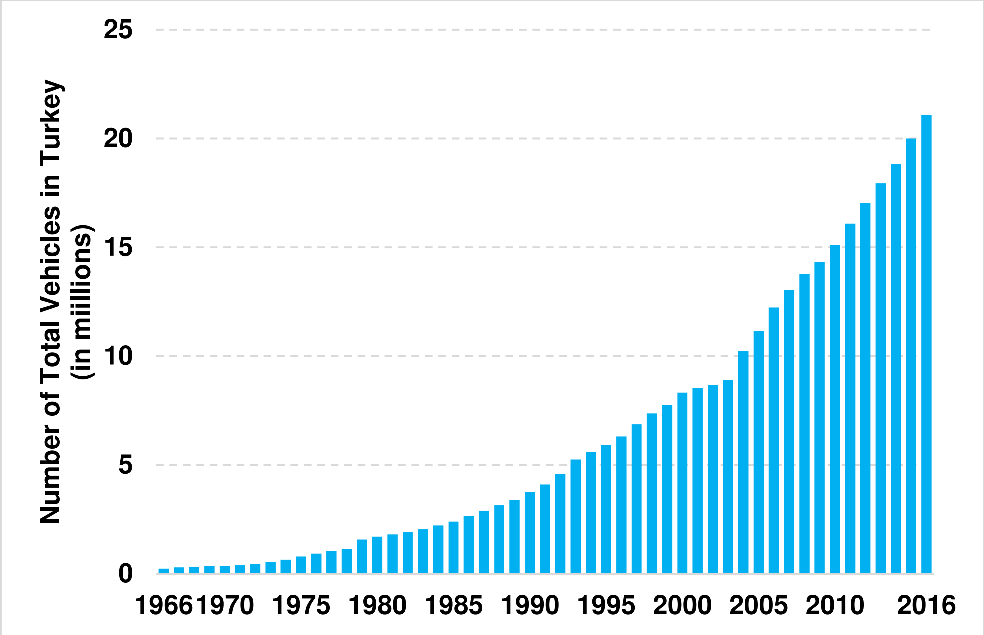

Figure 1.4. Number of total vehicles in Turkey, 1966-2016 (TUIK, 2017)

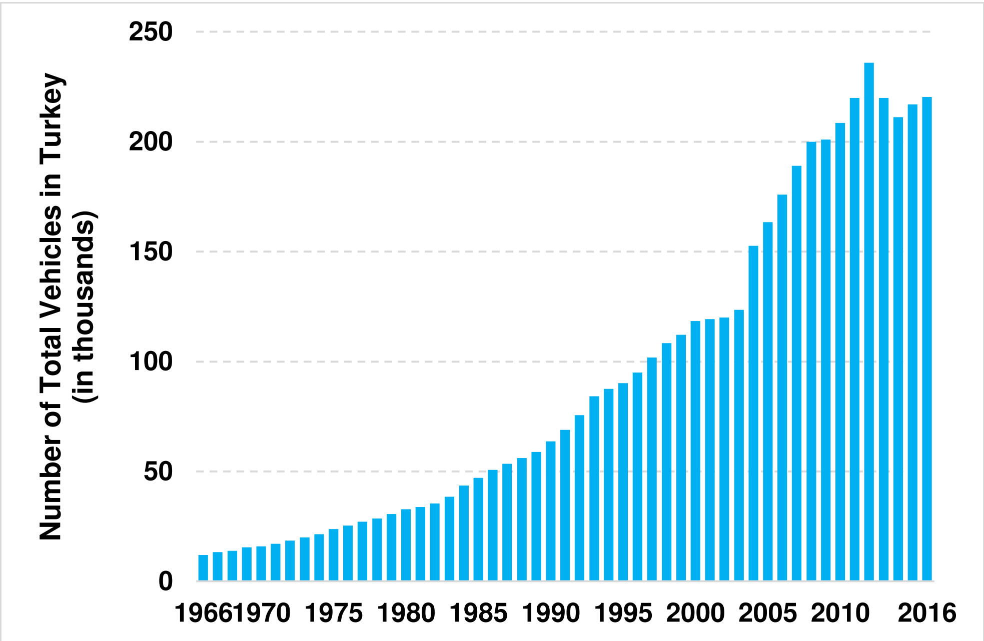

Figure 1.5. Number of total buses in Turkey, 1966-2016 (TUIK, 2017)

Automotive air conditioning (AAC) systems are the second largest energy consumers in vehicles including buses (Weilenmann, Alvarez and Keller, 2010). To reduce fuel consumption of an inter-city bus, increasing the energy efficiency of the ICBAC system should take into consideration.

With steady temperature increase throughout the years, the importance of AC systems is becoming more important part of our lives day by day. AC systems have great importance in transportation as well. The comfort of the passengers is as important as the energy efficiency of vehicles. An ideal AAC system reduces heat and humidity which can impact on our thermal comfort and air quality. The system also reduces dehydration level and thus excessive sweating (Chu and Jong, 2008). The importance of air conditioner becomes clearer, especially when hot temperatures being experienced. On the other hand, AAC systems and most of their components, regardless of their benefits, consume great amounts of energy. They are also inefficient for energy saving. The energy efficiency of AAC systems can be increased with many factor such as different MR, different refrigerant (Tosun, Bilgili, Tuccar and Aydın, 2016).

High energy efficiency can be achieved with high exergy efficiency and low exergy destruction values. The general definition of exergy is the maximum useful work that could be obtained from the system at a given state in a specified environment (Boles and Cengel, 2005). For instance, this can be achieved with maximum obtainable power for turbine, and minimum power transmission for pumps and compressors. Figure 1.6 shows the interdisciplinary triangle covered by the field of exergy analysis. It is demonstrated in the figure that energy, environment and sustainable development are the main factors that affect the exergy analysis.

There are several available refrigerants for AC systems. R404A, R410A, R502, R507, R22, R290, R134a, R500 and, R600a refrigerants are some of them. All of them have some small differences that matters to manufacturers. R134a and R600a are commonly used examples of these refrigerants. In this thesis, calculated exergy analysis of selected refrigerants for an ICBAC system will be focused primarily.

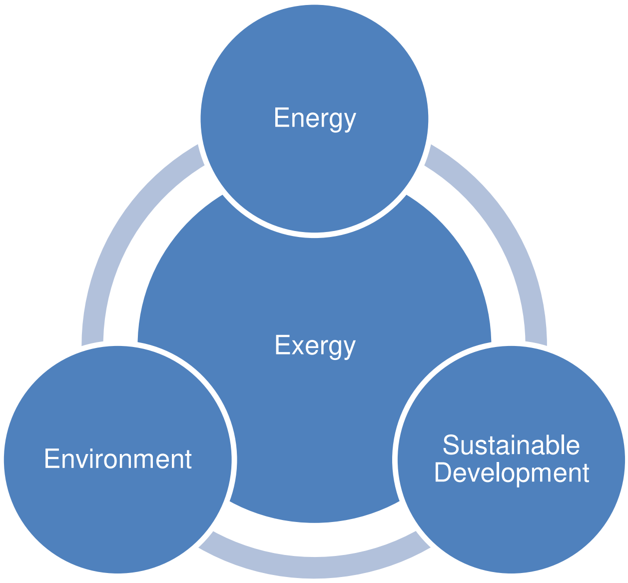

Figure 1.6. Interdisciplinary triangle covered by the field of exergy analysis (Tobergte and Curtis, 2013)

The aim of this thesis is to perform energy and exergy analysis using different refrigerants and MRs to enhance the efficiency of the ICBAC system. In this regard, Adana province of Turkey was chosen as the study region. A coach bus, which is used for inter-city passenger transportation, was selected. HAP was used to determine the hourly cooling load capacity of the selected inter-city bus model. Then, refrigerants were selected for use in the ICBAC system. Lastly, obtained COP, exergy efficiency and exergy destruction values of the ICBAC system and its components were evaluated and discussed in detail.

2. PRELIMINARY WORK

There are numerous studies related to energy and exergy analysis of the residential and automotive air conditioning systems with different refrigerants.

2.1. Energy and Exergy Analysis on Various Studies

Kaushik et al. made an extensive analysis of various studies related to energy and exergy analyses of thermal power plants through years. According to the exergy analysis, the main energy loss of a coal based thermal power plant, and a gas fired combined cycle thermal power plant occurred in boiler and combustion chamber, respectively. It is also stated that the efficiency of various plant components can be enhanced by expanding their size (Kaushik, Reddy, and Tyagi, 2011).

Rana and Mehta calculated the turbine heat rates, energy efficiency, exergy efficiency and exergy destructions of a steam turbine with different set of maximum continuous rating (MCR) condition values. The study revealed that steam turbine at 80 % MCR enhanced plant heat rate by 1356.72 kJ/kWh, which resulted in reduction of environmental CO_2 emission, ash generation and SO_2 emission by 1907.79 kg/h, 122.58 kg/ h and 43.66 kg/h, respectively (Rana and Mehta, 2013).

Ozdil et al. studied a complete thermodynamic analysis of an organic Rankine cycle (ORC) in the steel industry using a real plant data and performance cycle. The analysis of components including an evaporator, a condenser, a turbine demonstrated that it should be primarily focused on the evaporator inspection to enhance the performance of the entire system (Tumen Ozdil, Segmen and Tantekin, 2015).

Ozdil et al. examined the energy and exergy analyses of a 6.5 MW power plant system. The system, which includes a fluidized bed coal combustor (FBCC), a heat recovery steam generator and the FBCC, has the highest amount of irreversibility due to the high excess air value. The results showed that inadequate combustion efficiency in FBCC could be increased with reducing excess air amount. Additionally, fuel with a better calorific value could be used to increase efficiency in FBCC (Tumen Ozdil, Tantekin and Erbay, 2016).

Gürtürk and Oztop implemented the energy and exergy analysis of a cogeneration power plant. Their study focused on the circulation fluidized bed boiler (CFBB) which is the most essential section of the plant. Energy and exergy efficiency of the CFBB were calculated as 84.65% and 29.43% which is below than average value, respectively. The results indicated that project parameters must be revised and CFBB must be improved (Gürtürk and Oztop, 2016).

Ozdil and Segmen examined the exergoeconomic analysis of an ORC power plant. Four different water phases are considered to observe the influence of the water phase in the evaporator inlet on both exergoeconomic factor and economic system performance. According to the results, evaporator inlet phase in saturated liquid form has a greater exergoeconomic performance. Furthermore, the payback period of the plant is estimated as 3.27 years (Tumen Ozdil and Segmen, 2016).

2.2. Studies on Automotive Air Conditioning Systems

Mansour et al. studied a novel control strategy to enhance energy efficiency of a bus AC system operated in hot humid areas. Compared to the existing systems, the adopted control strategy has a higher energy efficiency and thermal comfort on many partial load scenarios. Additionally, payback period of the system was calculated as 17 months. The economic analysis showed that the system life cycle cost would be reduced by 20% with the proposed system (Khamis Mansour, Musa, Wan Hassan and Saqr, 2008a).

Mansour et al. made a thermoeconomic optimization of a finned-tube evaporator configuration of AC system of a bus. This method included the examination of the chosen parameters effects on the evaporator configuration design. In comparison to the currently used finned-tube evaporator, a remarkable improvement could be achieved with the proposed design parameters (Khamis Mansour, Musa, Wan Hassan and Saqr, 2008b).

Shek and Chan analyzed a combined comfort model of thermal comfort and air quality of AAC systems on buses. Combined comfort models were designed with the examination of the relationship between the subjective and objective data. AC setting adjustments could be controlled and transmitted to the hardware by processing the received data. It can be concluded that the developed model could help to optimize AC control by creating an important balance between passengers comfort and energy efficiency (Shek and Chan, 2008).

Bobbo et al. studied the application of R1234yf as a replacement of R134a in AAC systems. As it was stated with a European Parliament and of the Council Directive that after the beginning of 2011, the fluorinated greenhouse gases with high GWP usage was prohibited in automotive applications. High GWP R134a, which is commonly used in the automotive applications, should be replaced by refrigerants with lower GWP. Low GWP R1234yf which has thermodynamic properties similar to R134a has been suggested as an alternative refrigerant. The usage of R1234yf as a primary refrigerant was being debated at the time of study (Bobbo, Zilio, Scattolin and Fedele, 2014).

Datta et al. made an experimental study to calculate the performance of a cross-flow, microchannel condenser of an AAC system which was exposed to the unevenly distributed airflow. Project environment has been arranged by positioning screens with various shapes and blockage areas. Condenser cooling performance under blocked condition was monitored by infrared imaging. Although the performance of the condenser was decreased noticeably, the refrigerant flow increased in parallel with to blockage area. Compared to the regular operating condition, COP and cooling capacity of the system having a blockage area of 50% was decreased by 16.8% and 8.16%, respectively (Datta, Das, and Mukhopadhyay, 2014).

Ng et al. made an experimental study on the usage of an adaptive neural predictive control for AAC system. Dynamics of the system was defined by a Heating, Ventilating, and Air Conditioning (HVAC) model. In comparison to the previous situation, AAC system with offered neural predictive control has higher performance of disturbance rejection and reference tracking (Ng, Darus, Jamaluddin and Kamar, 2014a).

Ng et al. conducted an experiment study of a nonlinear autoregressive exogenous (NARX) model. NARX was suggested to demonstrate the dynamic behavior of an AAC system equipped with different speed compressors. Multilayer perceptron (MLP) and radial basis network (RBN) were used as network architectures under arbitrary compressor speed to simulate the varied cabin temperature. The calculation showed that MLP model were more desirable than RBN due to better performance (Ng, Darus, Jamaluddin and Kamar, 2014b).

Solmaz et al. studied hourly cooling load prediction in automotive industry using artificial neural network (ANN). It was calculated along the cooling season of the southern Turkey. The model was determined with seven neurons. The results revealed that the cooling load of a vehicle can be realistically estimated by ANNs from meteorological data and geographical characteristics (Solmaz, Ozgoren and Aksoy, 2014).

Sharafian and Bahrami investigated adsorber bed designs in waste-heat driven adsorption cooling systems. The former studies were categorized into nine groups with respect to their adsorber beds for AAC and refrigerant utilizations. The results showed that optimization of fin height and fin spacing, and improving thermal conductivity of adsorbent material by adding metal wool inside the finned tube adsorber bed are offered as the convenient solutions. Thus, it would enhance mass transfer and heat rates within the adsorber bed (Sharafian and Bahrami, 2014).

Zhang and Canova made a study on tracking performance of AAC system via μ synthesis. Model uncertainties on robust performance and stability were examined with the concept of the structured singular μ value. Compared to H∞ methods, performance and stability of the AAC system were improved with μ synthesis. It was also concluded that the μ controller has better performances of disturbance rejection and output tracking than the H∞ controller for the reviewed AAC system (Zhang and Canova, 2015a).

Sukri et al. investigated the different approaches of achieving a high energy-efficient ACC system for vapor compression refrigeration cycle. At the time of the study, some of the technologies and strategies specified were only conceptual. The increasing demand for an energy efficient AAC system has naturally resulted in more studies in order to design more efficient systems (Sukri, Musa, Senawi and Nasution, 2015).

Unal studied to determine optimum ejector dimension of AAC system. Two phase ejector was selected using R134a as a refrisgerant. Presumed cooling loads of bus and midibus are 32 kW and 14 kW, respectively. After thermodynamic analyses was performed, optimum overall length of two phase ejectors were calculated as 793.1 mm and 480.8 mm for bus and midibus (Ünal, 2015).

Yilmaz studied transcritical organic Rankine vapor compression (T-ORVC) refrigeration system for ICBAC system recovering engine exhaust heat. In that study, dry refrigerant R245fa and wet refrigerant R134a were considered as refrigerants. It is obtained that cooling load of 30 kW for an inter-city bus using T-ORVC system can be achieved utilizing engine exhaust waste heat energy (Yilmaz, 2015).

Suh et al. experimentally analyzed of HVAC system of an electric bus with dynamic wireless charging capability to create an efficient system design. An integrated HVAC system was proposed to achieve the efficiency which is vital for all vehicles, especially electric buses (Suh, Lee, Kim, Oh, and Won, 2015).

Unal and Yilmaz studied thermodynamic analysis of the two-phase ejector AC system powered by bus engines. It was presumed that the mixing process in ejector took place at constant pressure and fixed cross-sectional area. Depending on design parameters of the bus AC system, COP improvement can be achieved up to15% by using two phase ejector as an expansion device (Ünal and Yilmaz, 2015).

Zhang and Canova simulated an AAC system with storage evaporator to improve the automotive energy management. Calculations were implemented with MATLAB software. Hence, Phase Change Material is used in an innovational storage evaporator to increase the performance of AAC system. The study showed that results were encouraging to generalize the method for other designs (Zhang and Canova, 2015b).

Schulze et al. performed a transient evaluation of a city bus AC system with R-445a as a refrigerant. Usage of R-445a as a drop-in solution for R134a under similar environmental condition was investigated. It is concluded that it could lead to a COP enhancement and a significant amount of cooling capacity reduction over the operation time (Schulze, Raabe, Tegethoff, and Koehler, 2014).

Ali and Chakraborty simulated the thermodynamic modelling and performance of an engine waste heat driven adsorption cooling for AAC. The results indicated that the exhaust energy of a six cylinder 3000 cc private car is able to generate approximately 3 kW of cooling power for the car cabin. Hence, it was noticed that the heat source temperature was unstable during the cycle time unlike the conventional adsorption chiller. The hot water temperatures were ranged from 65 to 95 °C. It could be concluded that $CaCl_2$-in-silica gel was the ideal candidate for vehicle air cooling applications due to its higher COP and specific cooling power with small adsorption reactors (Ali and Chakraborty, 2015).

2.3. Energy and Exergy Analysis of Air Conditioning Systems

Kalaiselvam and Saravanan made an exergy analysis of scroll compressors working with three different refrigerants for HVAC system. Irreversibility and thermodynamical behavior of studied refrigerants R22, R417A, and R407C were examined in an AC system. The results indicated R417a could be used as a replacement of R22 (Kalaiselvam and Saravanan, 2009).

Sun et al. examined the energy and exergy analysis of multi-functional heat pump and conventional heat pump systems (MHPS). Additionally, studied system was compared to the conventional heat pump AC systems. The performances of the main system components were also analyzed to achieve an efficient MHPS design (Sun, Wu, and Wang, 2013).

Aprea et al. made a replacement study of high GWP refrigerant R134a with refrigerant R744. The exergy analysis of two refrigerants was implemented based on experimental data. The results showed that the total exergy efficiency of the conventional vapor compression plant operating with R134a were higher than R744 at all conditions, varying from 20 to 44% (Aprea, Greco, and Maiorino, 2013).

Bilgili et al. investigated the energy and exergy efficiency of a typical residential split AC system. Experimental studies were realized with different outdoor temperatures. The results proved that the increment in outdoor temperature influenced the overall system performance and performance of system components significantly (Bilgili, Ozbek, Yasar, Simsek, and Sahin, 2016).

Ozbek made an exergy analysis of a ceiling-type residential AC system working under various climatic conditions. The hourly cooling load capacities of a reference building during the months from April to September were calculated using HAP. The calculation indicated that lower atmospheric temperature affected the performance of the system and all system components (Ozbek, 2016b).

Ozbek realized an exergy analysis of a ceiling-type residential AC system working under different refrigerants. The hourly cooling load capacities of a reference building during months from April to September were calculated using HAP. The results showed that refrigerant R600a has a lower exergy destructions in the condenser, compressor and capillary compared to R404A, but the exergy destruction values in the evaporator didn’t affected significantly (Ozbek, 2016a).

2.4. Energy and Exergy Analysis of Automotive Air Conditioning Systems

Hosoz and Direk studied experimentally the exergy analysis of an R134a automotive HVAC system using environmental air as a heat source. Results indicated that this method with additional low cost components and with negligible packaging adjustments could be an ideal solution to the inadequate comfort heating for energy efficient vehicles (Hosoz and Direk, 2006).

Hosoz and Direk examined the energy and exergy analysis of a vehicle heat pump system operating with R134a and environmental air as a heat source. The analysis showed that the heat pump could be used as an additional source to the main system of a vehicle producing inadequate waste heat (Direk and Hosoz, 2008).

Alkan and Hosoz made an experimental study on ACC system with a variable capacity compressor using different mechanical instruments. Results indicated that speed of compressor increased with cooling capacity. Moreover, the exergy destruction rate of the system increased and the COP reduced with increasing speed of compressor (Alkan and Hosoz, 2010b).

Alkan and Hosoz carried out an experimental study on exergy performance of AAC with variable and fixed capacity compressors. Steady-state operating conditions were used by altering the compressor speed for each compressor state. The study indicated that the value of exergy destruction rate remained nearly uniform in variable capacity compressors (Alkan and Hosoz, 2010a).

Li et al. made an experimental study of energy and exergy performance of secondary loop systems (2LPs) using refrigerants with low GWP. A direct expansion system with R134a was used as a baseline system in comparison with these 2LPs. As compared to the baseline system, the total exergy destruction was decreased approximately 9.6% for the HFC-152a 2LP and 14.3% for the HC-290 2LP (Li, Eisele, Lee, Hwang, and Radermacher, 2014).

Tosun et al. performed an exergy analysis using different MRs to enhance the ICBAC system efficiency. Adana province of Turkey was chosen as the study region. Firstly, a coach bus, which is used for inter-city passenger transportation in USA, with a passenger capacity of 56 persons is selected. HAP was used to determine the hourly cooling load capacity of the selected inter-city bus model. In cooling load calculation of the inter-city bus, climate data such as dry bulb temperature, wet bulb temperature and solar radiation of the Adana province were used. The results showed that performance of the ICBAC system was affected significantly from MRs and outdoor temperatures. Maximum obtained exergy destruction values occurred at MR=0.5 for July. Exergy destruction values were determined as 2.61 kW, 0.99 kW and 2.78 kW for condenser, expansion valve and evaporator, respectively. (Tosun et al., 2016).

3. MATERIAL AND METHOD

3.1. Cooling Load Analysis

Cooling load (heat gain) calculation is essential to design and select the components of a HVAC system. Each heat gain realized by an inter-city bus under defined conditions must be considered for cooling load design (Tosun et al., 2016). The generated heat of total cooling load is originated by equipment, appliances, passengers and lights, and heat transferred through the selected inter-city bus envelope, including front and rear bodies, side panels, roof, windows, doors, floor, etc. The heat transfer rate through opaque surfaces, some of which are side front and rear bodies, roof, side panels, floor can be calculated as:

$$\mathrm{Q_{opaque} = U_{opaque} \cdot A_{opaque} \cdot CLTD} \tag{3.1}$$

where $\mathrm{U_{opaque}}$, $\mathrm{A_{opaque}}$ and CLTD are the overall heat transfer coefficient, the heat transfer area of the surface on the side of selected inter-city bus and cooling load (heat gain) temperature difference, respectively. Moreover, the heat transfer through glass can be calculated as:

$$\mathrm{Q_{glass} = A_{glass} \cdot \left[U_{glass} \cdot (T_o - T_i) + SHGF_{max} \cdot SC\right]} \tag{3.2}$$

where $\mathrm{A_{glass}}$, $\mathrm{U_{glass}}$, T_o and T_i are glass area, glass heat transfer coefficient, the outdoor and indoor air temperatures, respectively. The abbreviation for maximum solar heat gain factor is $\mathrm{SHGF_{max}}$. Besides, the shading coefficient is displayed with SC. The transfer rates of sensible heat and latent heat by virtue of the by-pass ventilation are given by:

$$\mathrm{\dot{Q}_{s,by-pass} = \dot{m}_o \cdot BPF \cdot c_p \cdot (T_o - T_i)} \tag{3.3}$$

$$\dot{Q}_{l,by-pass} = \dot{m}_o \cdot BPF \cdot h_{fg} \cdot (w_o - w_i) \tag{3.4}$$

where, $\dot{m}_o$, c_p and BPF are the mass flow rate of outdoor air, specific heat of moist air and the by-pass factor, respectively. The latent heat of vaporization is h_{fg}. Moreover, w_o and w_i are the humidity ratios of outdoor and indoor air, respectively. Besides these external loads, there are also inertial loads resulting from passengers, equipment, lighting, appliances and lighting. Lastly, the sensible cooling load, $\dot{Q}_{sensible,bus}$, the latent cooling load, $\dot{Q}_{latent,bus}$, and total cooling load, $\dot{Q}_{total,bus}$, on the inter-city bus can be calculated as (Tosun et al., 2016):

$$\begin{aligned}\dot{Q}_{sensible,bus} = {} & \dot{Q}_{glass} + \dot{Q}_{opaque} + \dot{Q}_{s,by-pass} + \dot{Q}_{s,infiltration} \\ & + \dot{Q}_{s,occupants} + \dot{Q}_{s,appliances} + \dot{Q}_{s,lighting}\end{aligned} \tag{3.5}$$

$$\dot{Q}_{latent,bus} = \dot{Q}_{l,by-pass} + \dot{Q}_{l,infiltration} + \dot{Q}_{l,occupants} + \dot{Q}_{l,appliances} \tag{3.6}$$

$$\dot{Q}_{total,bus} = \dot{Q}_{sensible,bus} + \dot{Q}_{latent,bus} \tag{3.7}$$

3.2. Air Conditioning System Analysis

A schematic view of the ICBAC system is displayed on Figure 3.1. As presented in the figure, the outside fresh air is firstly mixed with re-circulated air to satisfy the ventilation requirement. Then, the mixed air flows through a cooling coil (evaporator), and it is supplied to the cabin by the evaporator fan. The AC is supplied by vapor compression refrigeration cycle. A standard ICBAC system components are compressor, evaporator, expansion valve and condenser. Standard systems generally use an open-shaft compressor, which is powered by belt driven from the bus diesel engine. An electrically operated clutch which controls the compressor to supply adequate amount of air to the AC system is also used.

The mass flow rate of outdoor air, $\dot{m}_o$, and the mass flow rate of indoor air, $\dot{m}_i$, are mixed at a constant pressure and certain rate. The value of MR given by:

$$MR = \frac{\dot{m}_o}{\dot{m}_i} \tag{3.8}$$

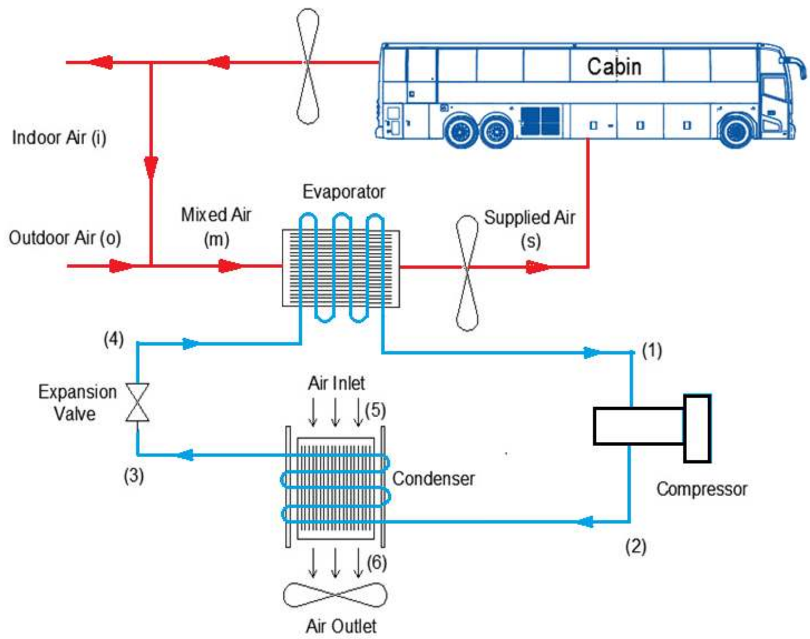

Figure 3.1. Schematic view of the ICBAC system

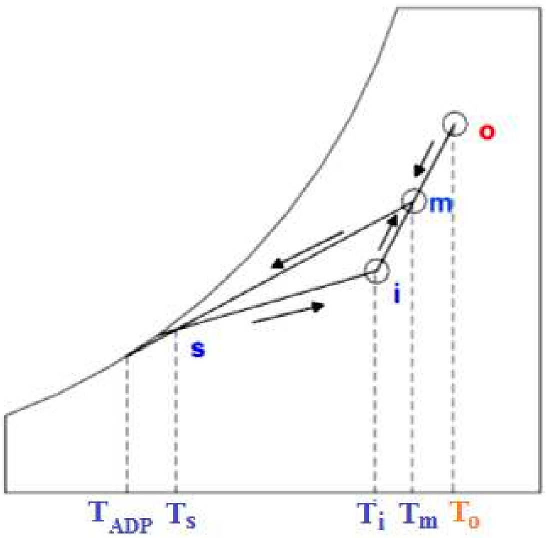

Figure 3.2. The schematic diagram of the ICBAC system with outdoor air and the corresponding process on psychometric chart

The schematic diagram of the ICBAC system with outdoor air and the corresponding process on psychometric chart is shown in Figure 3.2. As shown from the figure, the mass balance and energy balance must be taken into account to determine the mass flow rate of mixed air, $\dot{m}_s$, and its thermodynamic properties. From the mass balance of dry air and water vapor:

$$\dot{m}_s = \dot{m}_o + \dot{m}_i = \dot{m}_m \tag{3.9}$$

$$\dot{m}_m \cdot w_m = \dot{m}_o \cdot w_o + \dot{m}_i \cdot w_i \tag{3.10}$$

From the energy balance:

$$\dot{m}_m \cdot h_m = \dot{m}_o \cdot h_o + \dot{m}_i \cdot h_i \tag{3.11}$$

The sensible cooling load, $\dot{Q}_{sensible,bus}$, and the latent cooling load,

$\dot{Q}_{latent,bus}$, on the inter-city bus can be defined as:

$$\dot{Q}_{sensible,bus} = \dot{m}_s \cdot c_p \cdot (T_i - T_o) \tag{3.12}$$

$$\dot{Q}_{latent,bus} = \dot{m}_s \cdot h_{fg} \cdot (w_i - w_o) \tag{3.13}$$

By-pass factor, BPF can be calculated as:

$$BPF = \frac{T_s - T_{ADP}}{T_m - T_{ADP}} \tag{3.14}$$

where T_s, T_{ADP} and T_m are the supplied air temperature, the coil apparatus dew-point temperature and the mixed air temperature, respectively. The optimum capacity of the cooling coil, $\dot{Q}_{evaporator}$, can be obtained from energy balance across the cooling coil:

$$\dot{Q}_{evaporator} = \dot{m}_s \cdot (h_m - h_s) - \dot{m}_w \cdot h_w \tag{3.15}$$

where h_w and $\dot{m}_w$ are the enthalpy of condensate leaving the cooling coil (evaporator) and mass flow rate of condensate on the coil, respectively. $\dot{m}_w$ can be calculated as follows:

$$\dot{m}_w = \dot{m}_s \cdot (w_m - w_s) \tag{3.16}$$

3.3. Refrigeration System Analysis

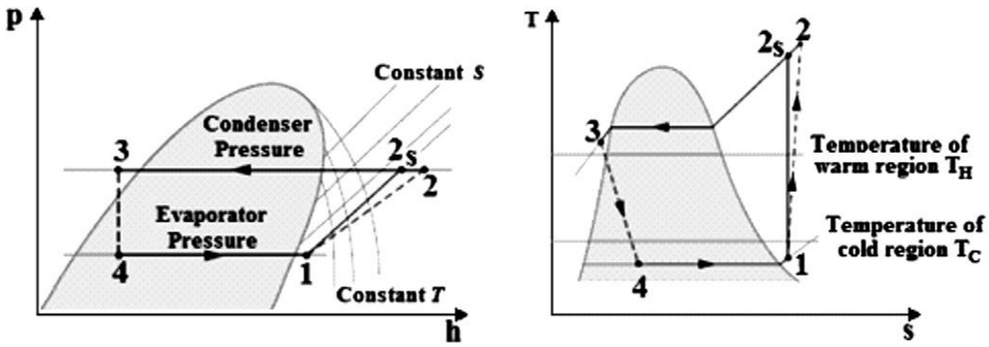

Figure 3.3. P-h (Pressure-enthalpy) and T-S (Temperature-entropy) diagrams of vapor-compression cycle for ICBAC systems (Bilgili, 2011)

Pressure-enthalpy and temperature-entropy diagrams of vapor compression cycle of the ICBAC system are presented in Figure 3.3. The energy balance of steady state process are shown as:

$$\dot{E}_{in} = \dot{E}_{out} \tag{3.17}$$

where the subscript "in" and "out" represents the rate of net energy transfer in and out by heat, work and mass, respectively. It should be considered that energy can only be transferred by heat, $\dot{Q}$, work, $\dot{W}$, and mass, $\dot{m}$. Alternatively, the energy balance for a general steady-flow system is defined as (Yamaguchi et al., 2016):

$$\dot{Q}_{in} + \dot{W}_{in} + \sum_{in} \dot{m} \cdot \left(h + \frac{V^2}{2} + g \cdot z \right) = \dot{Q}_{out} + \dot{W}_{out} + \sum_{out} \dot{m} \cdot \left(h + \frac{V^2}{2} + g \cdot z \right) \tag{3.18}$$

where h and V are the enthalpy per unit mass and velocity of the system relative to some fixed reference frame, respectively. Additionally, z is abbreviation for the elevation of the center of gravity of a system relative to some arbitrarily selected reference level. Besides, the specific enthalpy at the compressor exit (state 2), h_2, is given by (Bilgili, 2011):

$$h_2 = h_1 + \frac{h_{2s} - h_1}{\eta} \tag{3.19}$$

where the specific enthalpy at state 2s is shown as h_{2s}. Furthermore, the compressor isentropic efficiency, η, can be expressed as (Ünal and Yilmaz, 2015):

$$\eta = 0.874 - 0.0135 \cdot \frac{P_{cond}}{P_{evap}} \tag{3.20}$$

Here, P_{cond} is the condenser pressure and P_{evap} is the evaporator pressure. The entropy balance relation for a general steady-flow process is written as (Yamaguchi et al., 2016):

$$\dot{S}_{gen} = \sum \dot{m}_e \cdot s_e - \sum \dot{m}_i \cdot s_i - \sum \frac{\dot{Q}_k}{T_k} \tag{3.21}$$

where s is the entropy, $\dot{S}_{generation}$ is the entropy generation, and T_k is the temperature at location k. The heat transfer rate through the boundary at T_k is displayed with $\dot{Q}_k$. The exergy destruction, $\dot{E}x_{dest}$, proportional to the entropy generated, $\dot{S}_{gen}$, can be determined as (Yamaguchi et al., 2016):

$$\dot{E}x_{dest} = T_0 \cdot \dot{S}_{gen} \tag{3.22}$$

where T_0 stands for dead-state temperature. In additionally, the assumption of entropy-change relation for ideal gases under the constant-specific heats, $c_{p,avg}$, must be calculated from the following equation:

$$s_2 - s_1 = c_{p,avg} \cdot \ln\frac{T_2}{T_1} - R \cdot \ln\frac{P_2}{P_1} \tag{3.23}$$

The general exergy balance is written as:

$$\dot{E}x_{in} - \dot{E}x_{out} = \dot{E}x_{dest} \tag{3.24}$$

where $\dot{E}x_{in} - \dot{E}x_{out}$ is the rate of net exergy transfer by work, heat and mass. Moreover, the rate of net exergy destruction is indicated with $\dot{E}x_{dest}$ in the equation above. The general exergy balance can also be written in the rate form as:

$$\dot{E}x_{heat} - \dot{E}x_{work} + \dot{E}x_{mass,in} - \dot{E}x_{mass,out} = \dot{E}x_{dest} \tag{3.25}$$

Besides, the rate of formation of the general exergy balance is evaluated as (Yamaguchi et al., 2016):

$$\sum(1 - \frac{T_0}{T_k}) \cdot \dot{Q}_k - \dot{W} + \sum(\dot{m}_{in} \cdot ex_{in}) - \sum(\dot{m}_{out} \cdot ex_{out}) = \dot{E}x_{dest} \tag{3.26}$$

where $\dot{W}$ and ex are the work rate and the flow (specific) exergy, respectively. Additionally, the properties at the reference (dead) state of P_0 and T_0 is shown as subscript zero. The specific flow exergy of refrigerant or air can be calculated from the following equation:

$$ex_{ref,air} = (h - h_0) - T \cdot (s - s_0) \quad (3.27)$$

The exergy rate is calculated as (Hürdoğan, Buyükalaca, Hepbasli, and Yılmaz, 2011):

$$\dot{E}x = \dot{m} \cdot (ex) \quad (3.28)$$

The exergy efficiency of various steady-flow devices, ψ, can also be expressed as:

$$\psi = \frac{\dot{E}x_{out}}{\dot{E}x_{in}} = \frac{\text{Exergy recovered}}{\text{Exergy supplied}} \quad (3.29)$$

COP_{ref} which is an energy-based efficiency measure of the refrigeration unit is calculated from the following equation (Weilenmann et al., 2010):

$$COP_{ref} = \frac{\dot{Q}_{evap}}{\dot{W}_{comp}} \quad (3.30)$$

The reversible power, $\dot{W}_{rev}$, can be defined as:

$$\dot{W}_{rev} = \dot{W}_{comp} - \dot{E}x_{dest} = \dot{E}x_{out,comp} - \dot{E}x_{in,comp} \quad (3.31)$$

where difference between minimum required power to be supplied to the compressor (useful work) is $\dot{W}_{comp}$ and the exergy destruction is $\dot{E}x_{dest}$.

Energy, entropy, exergy and mass balances and exergy efficiencies for the ICBAC system components are given in Table 3.1.

Table 3.1. Energy, entropy, exergy and mass balances and exergy efficiencies for the ICBAC system equipment (compressor, condenser, expansion valve, evaporator)

Component	Description	Formula
Compressor 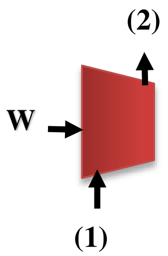	Mass Balance	$\dot{m}_1 = \dot{m}_2 = \dot{m}_{ref}$
	Energy Balance	$\dot{W}_{comp} = \dot{m}_{ref} \cdot (h_2 - h_1)$
	Entropy Balance	$\dot{S}_{gen,comp} = \dot{m}_{ref} \cdot (s_2 - s_1)$
	Exergy Balances	$\dot{E}x_{dest,comp} = \dot{m}_{ref} \cdot (ex_2 - ex_1) + \dot{W}_{comp}$
	Exergy Efficiency	$\psi_{comp} = \dfrac{\dot{E}x_2 - \dot{E}x_1}{\dot{W}_{comp}}$
Condenser 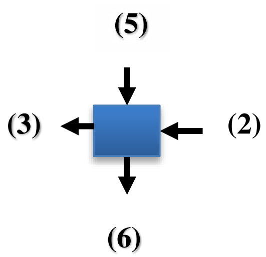	Mass Balance	$\dot{m}_2 = \dot{m}_3 = \dot{m}_{ref}; \quad \dot{m}_5 = \dot{m}_6 = \dot{m}_{air}$
	Energy Balance	$\dot{Q}_{cond} = \dot{m}_{ref} \cdot (h_2 - h_3) = \dot{m}_{air} \cdot c_{p,air} \cdot (T_6 - T_5)$
	Entropy Balance	$\dot{S}_{gen,cond} = \dot{m}_{ref} \cdot (s_3 - s_2) + \dot{m}_{air} \cdot \left(c_{p,air} \cdot \ln\dfrac{T_6}{T_5} - R \cdot \ln\dfrac{P_6}{P_5}\right)$
	Exergy Balances	$\dot{E}x_{dest,cond} = \dot{m}_{ref} \cdot (ex_2 - ex_3) + \dot{m}_{air} \cdot (ex_2 - ex_3)$
	Exergy Efficiency	$\psi_{cond} = \dfrac{\dot{m}_{air} \cdot (ex_6 - ex_5)}{\dot{m}_{ref} \cdot (ex_2 - ex_3)}$

Table 3.1. (Continued)

Component	Description	Formula
Expansion valve (3)  (4)	Mass Balance	$\dot{m}_3 = \dot{m}_4 = \dot{m}_{ref}$
	Energy Balance	$h_3 = h_4$
	Entropy Balance	$\dot{S}_{gen,exp.val.} = \dot{m}_{ref} \cdot (s_4 - s_3)$
	Exergy Balances	$\dot{E}x_{dest,exp.val.} = \dot{m}_{ref} \cdot (ex_3 - ex_4)$
	Exergy Efficiency	$\psi_{exp.val.} = \dfrac{\dot{m}_{ref} \cdot (ex_4)}{\dot{m}_{ref} \cdot (ex_3)}$
Evaporator (m) 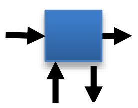 (s) (4) (1)	Mass Balance	$\dot{m}_1 = \dot{m}_4 = \dot{m}_{ref}; \quad \dot{m}_m = \dot{m}_s = \dot{m}_{air}$
	Energy Balance	$\dot{Q}_{evap} = \dot{m}_{ref} \cdot (h_1 - h_4) = \dot{m}_s \cdot (h_m - h_s) - \dot{m}_w \cdot h_w$
	Entropy Balance	$\dot{S}_{gen,evap} = \dot{m}_{ref} \cdot (s_1 - s_4) + \dot{m}_{air} \cdot \left(c_{p,air} \cdot \ln\dfrac{T_s}{T_m} - R \cdot \ln\dfrac{P_s}{P_m}\right)$
	Exergy Balances	$\dot{E}x_{dest,evap} = \dot{m}_{ref} \cdot (ex_4 - ex_1) + \dot{m}_{air} \cdot (ex_m - ex_s)$
	Exergy Efficiency	$\psi_{evap} = \dfrac{\dot{m}_{ref} \cdot ex_1 + \dot{m}_{air} \cdot ex_s}{\dot{m}_{ref} \cdot ex_4 + \dot{m}_{air} \cdot ex_m}$
Refrigeration unit (Figure 3.1)	**Overall Exergy Efficiency**	$\psi_R = \dfrac{\dot{E}x_{in,evap} - \dot{E}x_{out,evap}}{\dot{W}_{comp}}$
	Total Exergy Destruction	$\dot{E}x_{dest,ttl} = \dot{E}x_{dest,comp} + \dot{E}x_{dest,cond} + \dot{E}x_{dest,exp.val.} + \dot{E}x_{dest,evap}$

4. RESULTS AND DISCUSSIONS

In order to perform the energy and exergy analysis of the ICBAC system, following procedures were carried out respectively.

- Determination of study region and climatic data,
- Selection of the inter-city bus and determination of its material properties,
- Calculation of hourly cooling load capacity of inter-city bus,
- Investigation of the air-conditioning system of the TS-45 inter-city bus,
- Energy analysis of inter-city bus air-conditioning system,
- Exergy analysis of inter-city bus air-conditioning system,

4.1. Determination of study region and climatic data

Adana province of Turkey was chosen as the study region. In calculation of the cooling load (heat gain) of the inter-city bus, climate data such as dry bulb temperature, wet bulb temperature and solar radiation of the Adana province were used. Monthly variation of dry bulb temperature (air temperature) and wet bulb temperature through the year is displayed in Figure 4.1. As demonstrated in the figure, atmospheric air temperature reaches its maximum value during July and August months.

Hourly variation of atmospheric air temperature between May and September is displayed on Figure 4.2. As shown in the figure, maximum atmospheric air temperature is observed at 15:00 during July and August months.

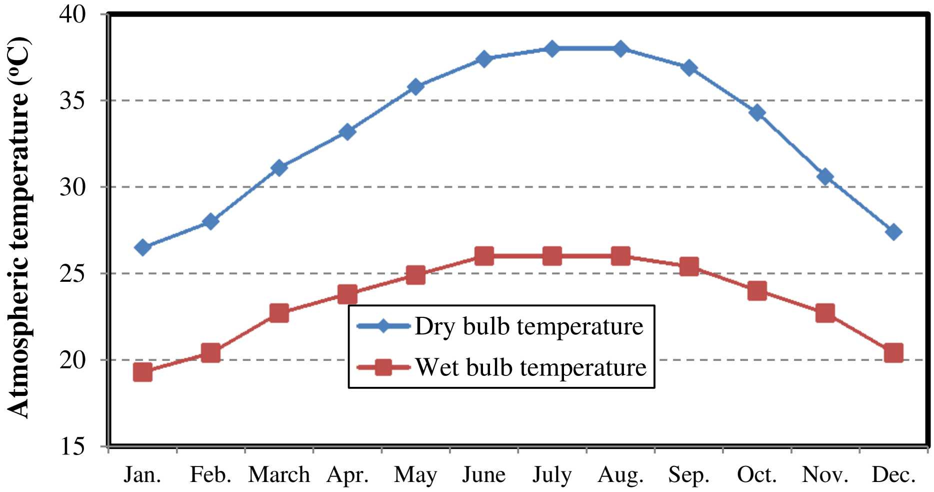

Figure 4.1. Monthly variation of dry bulb temperature and wet bulb temperature through the year

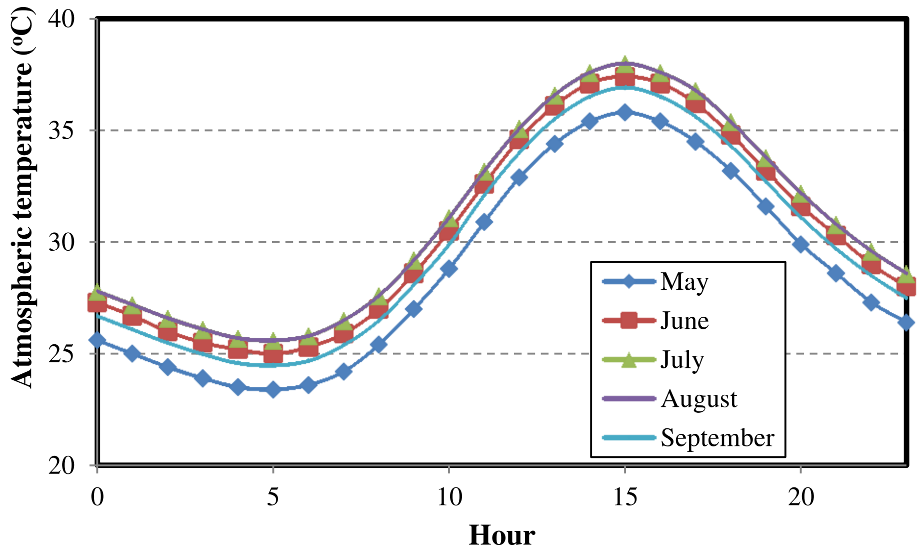

Figure 4.2. Hourly variation of atmospheric air temperature between May and September

4.2. Selection of the inter-city bus and determination of its material properties

The selected coach bus has a passenger capacity of 56 persons. In addition, the bus is used for inter-city passenger transportation in United States (CH Bus Sales, 2017).

General view of the TS 45 type inter-city bus belonging to TEMSA is shown in Figure 4.3, and dimensions of the inter-city bus are presented in Figure 4.4. The material properties of load components for space, envelope loads for space, heat transfer coefficient and surface area of the inter-city bus are given in Table 4.1. Dry bulb temperature and wet bulb temperature of outdoor air are accepted as 36.8 °C and 25.7 °C, respectively. The inter-city bus cabin is maintained at 24.4 °C dry bulb temperature and 50% relative humidity.

The TS45 type inter-city bus is constructed from stainless steel with an integral monocoque design that makes sure strength and stability. Moreover, the bus has a high capacity HVAC system with a 6 cylinder AC compressor, with brushless fans on evaporator and condenser, which ensures low operational and maintenance costs (CH Bus Sales, 2017).

Figure 4.3. General overview of the TS 45 type inter-city bus (CH Bus Sales, 2017)

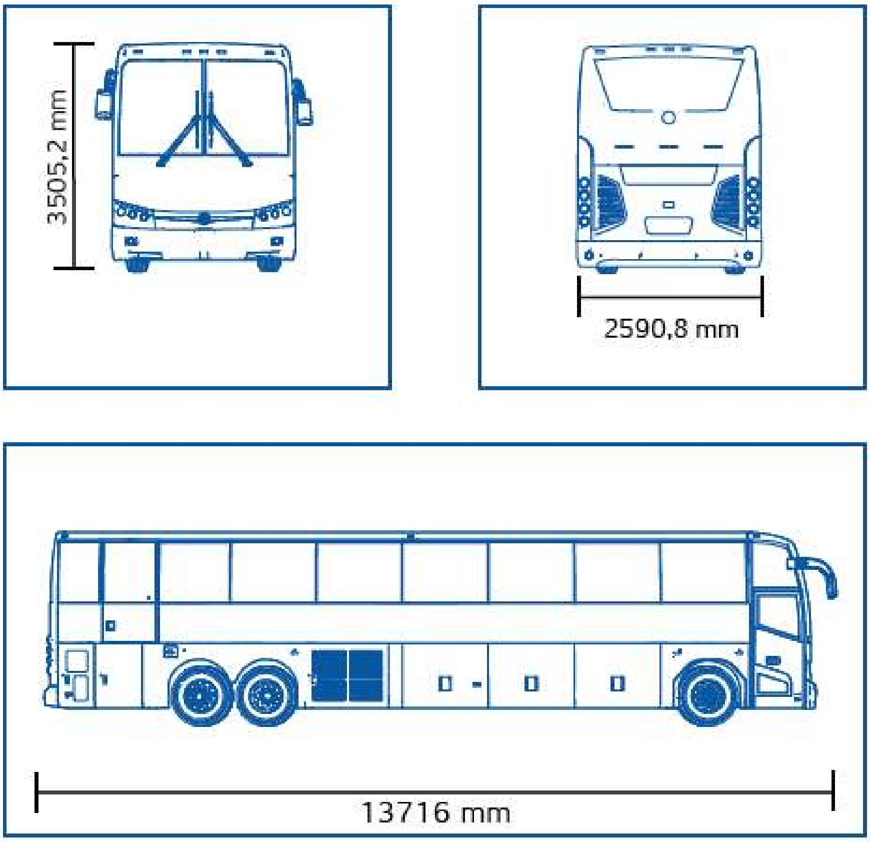

Dimensions of inter-city bus in mm (TEMSA)					
Length	**Width**	**Height**	**Wheelbase**	**Front Extension**	**Rear Extension**
13716	2590.8	3505.2	7894.3	1925.3	1925.3
Inter-city bus engine (CUMMINS)					
Model		CUMMINS ISX EPA13 345 HP			
Type		Diesel			
Number of Cylinders		6 in line			

Figure 4.4. Dimensions of the TS 45 type inter-city bus (Temsa, 2016)

Table 4.1. The material properties and space loads of the inter-city bus (Tosun et al., 2016)

a) Load components for space		Details	Sensible (W)	Latent (W)
Window and Skylight Solar Loads		35 m²	6162	-
Wall Transmission		28 m²	1891	-
Roof Transmission		32 m²	445	-
Window Transmission		35 m²	1145	-
Skylight Transmission		1 m²	42	-
Door Loads		0 m²	0	-
Floor Transmission		33 m²	796	-
Partitions		0 m²	0	-
Ceiling		0 m²	0	-
Overhead Lighting		0 W	0	-
Task Lighting		0 W	0	-
Electric Equipment		0 W	0	-
Number of People		56	3774	1971
Infiltration		-	0	0
Miscellaneous		-	0	0
Safety Factor		60% / 60%	8553	1183
Total Zone Loads		-	22808	3154
b) Envelope loads for space		**Area (m²)**	**U-Value W/(m²-K)**	**Shade coefficient**
West exposure	Side Panel	12	2.801	-
	Side Windows	13	2.569	0.811
	Door	2	4.890	0.811
East exposure	Side Panel	12	2.801	-
	Side Windows	13	2.569	0.811
	Driver Window	2	4.890	0.811
North exposure	Front Body	3	2.667	-
	Front Windows	2	5.020	0.811
South exposure	Rear Body	2	2.667	-
	Rear Window	3	2.611	0.811
Others	Roof	32	0.532	-
	Floor	33	2.267	-
	Skylight	1	4.890	0.811

4.3. Calculation of hourly cooling load capacity of inter-city bus

HAP is used to determine hourly cooling load capacity of the inter-city bus. This packet program is a computer tool which assists engineers in designing HVAC systems for residential, commercial and industrial buildings. Besides, it is quite useful for predicting cooling and heating loads, and thus designing systems. Moreover, it can be used for simulating energy use and determining energy costs. In this program, the ASHRAE-endorsed transfer function method and detailed 8760 hour-by-hour energy simulation techniques are used for load calculations and energy analysis (CARRIER, 2017).

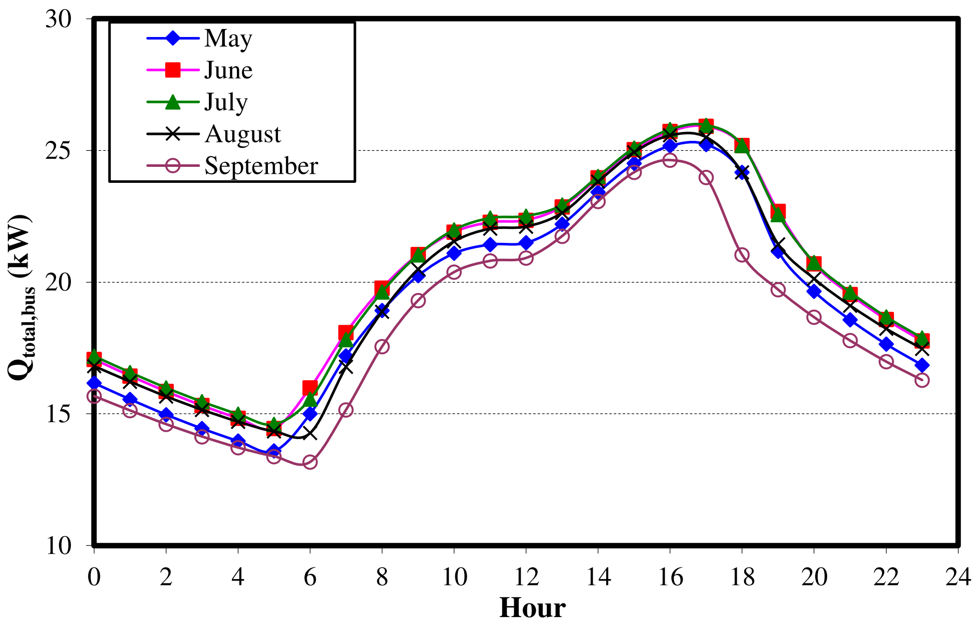

Figure 4.5. Hourly variations of the total cooling load on the inter-city bus between May and September

It was assumed that the inter-city bus was traveling to north direction at a speed of 120 km/h for the cooling load calculation. It was considered that heat transfer from the windows as a sensible heat gain takes place by conduction and convection, while heat transfer from the roof, floor, front, side and rear panels is realized only via conduction. Due to its minor value, heat transfer by infiltration was ignored. Furthermore, latent and sensible heat gains of occupants, by-pass ventilation air and appliances were determined. Lastly, the total cooling load (heat gain) on the inter-city bus was obtained from previous calculations.

Figure 4.5 presents the hourly variations of the total cooling load on the inter-city bus between May and September. As a consequence of change in the atmospheric air temperature and solar radiation, the total cooling load of the inter-city bus varies considerably during the day as presented in the figure. It can be observed from the figure that maximum heat gain values were computed to be nearly 25-26 kW and obtained at 17:00, while the minimum values were acquired at times when atmospheric air temperature and solar radiation were low. Maximum heat gain value was obtained as 25.96 kW at 17:00 in July. It was also the peak cooling load and peak time.

4.4. Investigation of the air-conditioning system of the TS-45 inter-city bus

3D view of the AC system of the TS45 inter-city bus is demonstrated in Figure 4.6, and schematic view of the ICBAC system is shown in Figure 4.10. As shown in these figures, circulating refrigerant vapor enters the compressor to be compressed to a higher pressure, causing increment in the refrigerant temperature. The hot refrigerant vapor with high pressure is discharged from compressor into the condenser. In condenser, refrigerant is cooled by air flowing across the condenser coils, causing its phase to change from gas to liquid. Hence, the heat of circulating refrigerant is taken away from the system by air.

Liquid refrigerant with high pressure passes through the expansion valve where it undergoes a rapid pressure reduction. The reduction in pressure causes flash evaporation of a part of the liquid refrigerant, thus causing reduction in refrigerant temperature. Afterwards, the cold refrigerant is routed through the evaporator. The hot air mixture of outdoor air and indoor air are blown through the evaporator. The process resulting in evaporation of the liquid part of the cold refrigerant mixture reduces the air mixture temperature further. Therefore, the hot air mixture is cooled. Lastly, the refrigerant vapor goes back into the compressor to repeat the cycle.

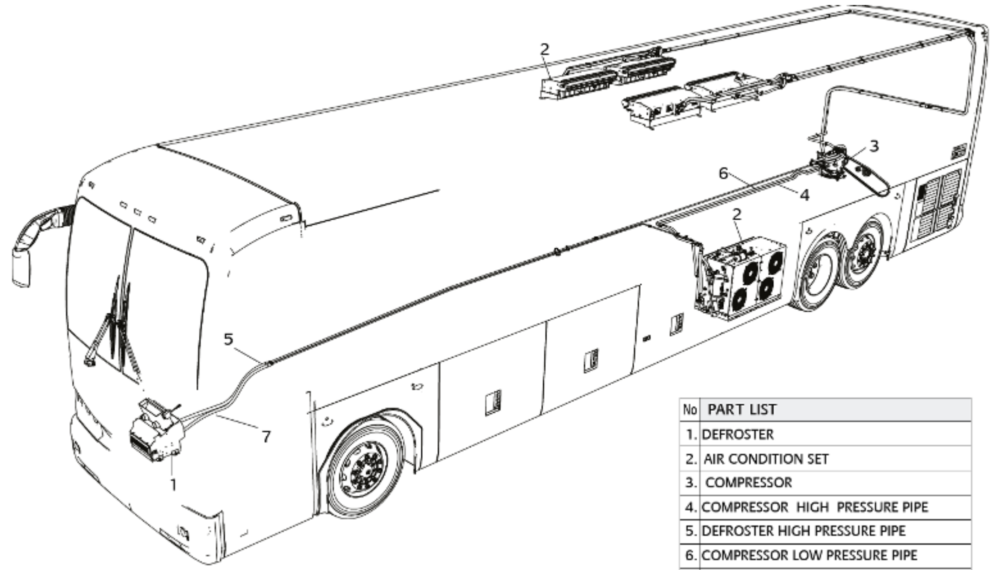

No	PART LIST
1.	DEFROSTER
2.	AIR CONDITION SET
3.	COMPRESSOR
4.	COMPRESSOR HIGH PRESSURE PIPE
5.	DEFROSTER HIGH PRESSURE PIPE
6.	COMPRESSOR LOW PRESSURE PIPE
7.	DEFROSTER LOW PRESSURE PIPE

Figure 4.6. 3D view of the AC system of TS45 Inter-City Bus (Temsa, 2016)

BUS	**TS45**
SUPPLIER	MCC
REFRIGERANT / R134a	12000
AC COOLING CAPACITY (kW)	48
AC HEATING CAPACITY (kW)	76
FRONT BOX COOLING CAPACITY (kW)	4.5
FRONT BOX HEATING CAPACITY (kW)	16

Figure 4.7. Capacities and charge amounts of the ICBAC system (Temsa, 2016)

Capacities and charge amounts of the ICBAC system are displayed in Figure 4.7. As seen in the figure, R134a is the currently used refrigerant in the refrigeration system. In addition, value of the given AC cooling capacity, 48 KW, will be compared with the calculated one in the following sections.

AC control unit of TS45 inter-city bus is displayed in the Figure 4.8, and service ports of AC system of TS45 inter-city is shown in Figure 4.9, respectively.

General features of these equipment can be obtained from these figures. As displayed in the figure 4.9, service ports are easily accessible from compressor and condenser areas for maintenance.

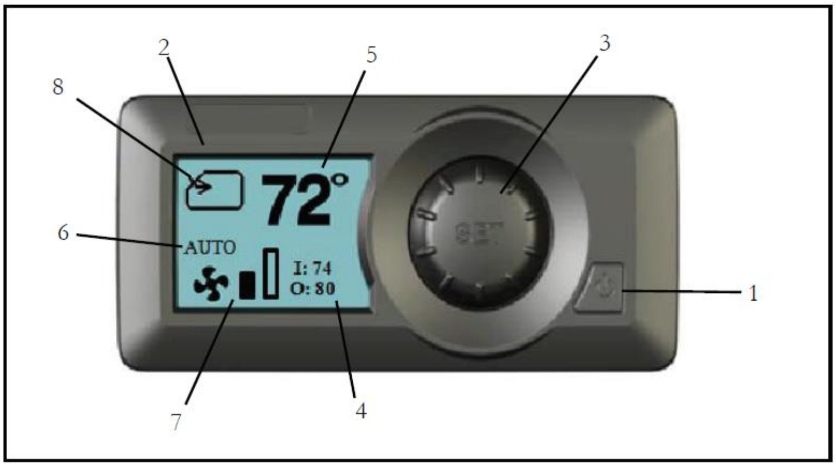

1. On/Off Button	5. Temperature Set Point
2. LCD Display	6. Mode of Operation
3. Set/Select Knob	7. Blower Speed
4 Inside/Outside Temperature	8. Fresh Air / Recirculation

Figure 4.8. AC control unit of TS45 inter-city bus (Temsa, 2016)

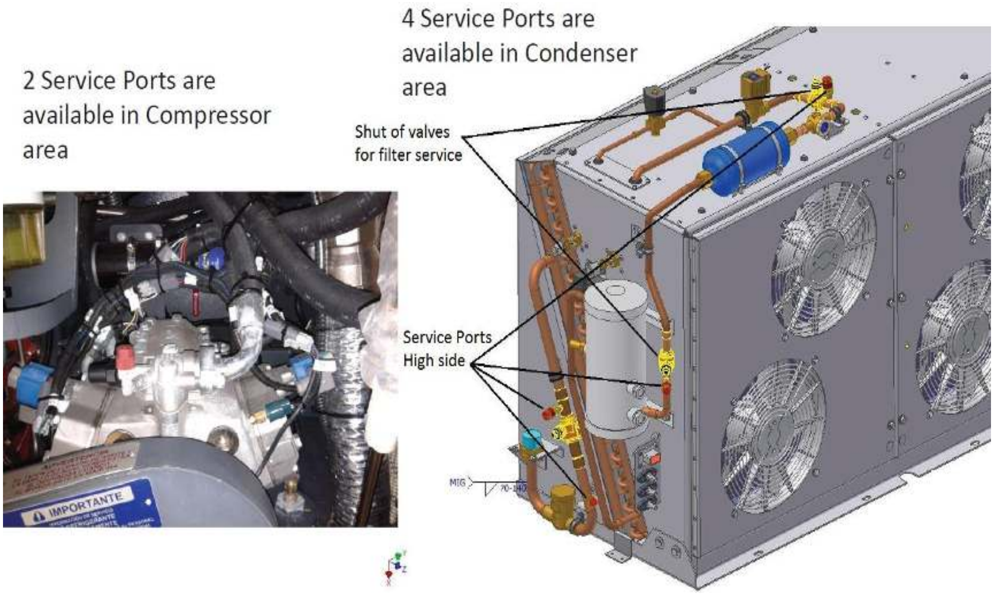

Figure 4.9. Service ports of the AC system of TS45 inter-city bus (Temsa, 2016)

4.5. Assumptions and analysis of the ICBAC system

As stated in Section 4.3, the maximum (peak) cooling load was determined at 17:00 in July. Therefore, the energy and exergy analysis of the ICBAC system were made considering the calculated peak load values. The MR value was considered to be between 0.05 and 0.5. Accordingly, the determined inside and outside design conditions and thermodynamic characteristics of the ICBAC system are given in Table 4.2.

A schematic view of the ICBAC system is shown in Figure 4.10. Furthermore, Figure 4.11 presents the ICBAC system with outdoor air for ventilation and the corresponding process on psychometric chart. As seen from these figures, to satisfy the ventilation requirement, outdoor air (o) is firstly mixed with indoor air (i) at a certain mass flow rate. Then, the mixed air (m) flows over the cooling coil (evaporator), where it is cooled and dehumidified. Lastly, the air (s) is supplied to the conditioned space.

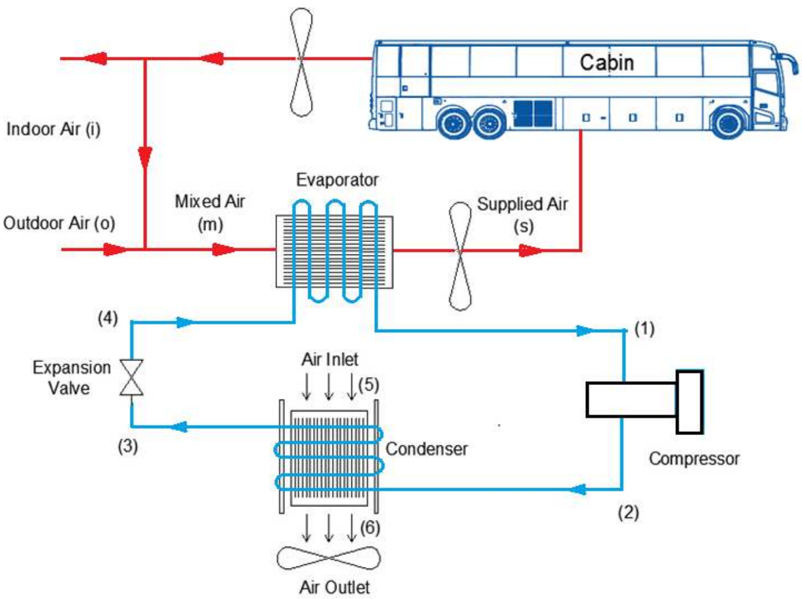

Figure 4.10. Schematic view of the ICBAC system

Table 4.2. Inside and outside design conditions and thermodynamic characteristics of the ICBAC system

Properties	**Unit**	**Value**
Dry bulb temperature of indoor air, T_i	°C	24.4
Wet bulb temperature of indoor air, $T_{i,wb}$	°C	17.4
Specific humidity of indoor air, w_i	kg/kg	0.00953
Enthalpy of indoor air, h_i	kJ/kg	48.82
Dry bulb temperature of outdoor air, T_o	°C	36.8
Wet bulb temperature of outdoor air, $T_{o,wb}$	°C	25.7
Specific humidity of outdoor air, w_o	kg/kg	0.01626
Enthalpy of outdoor air, h_o	kJ/kg	78.79
Sensible cooling load of the inter-city bus, $\dot{Q}_{sensible,bus}$	kW	22.808
Latent cooling load of the inter-city bus, $\dot{Q}_{latent,bus}$	kW	3.154
Total cooling load of the inter-city bus, $\dot{Q}_{total,bus}$	kW	25.962
Enthalpy of condensate water, h_w	kJ/kg	60.982
Dry bulb temperature of supply air, T_s	°C	14.4
Enthalpy of supply air, h_s	kJ/kg	36.67
Specific humidity of supply air, w_s	kg/kg	0.00884
Dry bulb temperature of mixed air, T_m	°C	28.53
Specific humidity of mixed air, w_m	kg/kg	0.01177
Enthalpy of mixed air, h_m	kJ/kg	58.810
Mass flow rate of supply air, $\dot{m}_s$	kg/s	2.233
Heat transfer on the cooling coil, $\dot{Q}_{coil}$	kW	49.030
Mass flow rate of condensate water, $\dot{m}_w$	kg/s	0.00654
Apparatus dew point temperature, T_{ADP}	°C	10.55
By-pass factor, BPF	-	0.2141
Air mixing ratio, MR	-	0.5

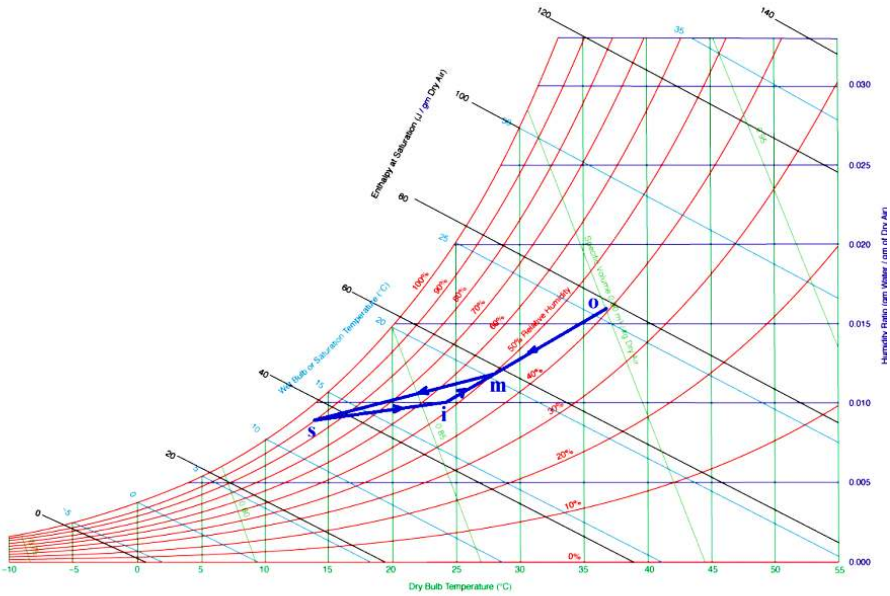

Figure 4.11. The ICBAC system with outdoor air for ventilation and the corresponding process on psychometric chart

The inter-city bus cabin is maintained at 24.4 °C dry bulb temperature and 50% relative humidity, while the outside design conditions are 36.8 °C dry bulb temperature and 25.7 °C wet bulb temperature. Outdoor air and indoor air were mixed at MR = 0.5, and the mixed air temperature was found to be 28.53 °C. The supplied air to the conditioned space was assumed to be 10 °C lower than the inside temperature, and thus determined as 14.4 °C.

The bus sensible heat gain ($\dot{Q}_{sensible,bus}$) value and the bus latent heat gain value ($\dot{Q}_{latent,bus}$) are determined as 22.808 kW and 3.154 kW. Moreover, the mass flow ($\dot{m}_s$), by-pass factor (BPF) and the apparatus dew point temperature (T_{ADP}) values were calculated as 2.233 kg/s, 0.2141 and 10.55 °C, respectively. In addition, the amount of heat transfer at evaporator and the amount of condensation on the evaporator surface were calculated as 49.030 kW and 0.00654 kg/s, respectively.

R404A, R410A, R502, R507, R22, R290, R134a, R500 and R600a were selected as different refrigerant types in the ICBAC system. Pressure-enthalpy (P-h) diagram of the ICBAC system for the sample refrigerant R134a is shown in Figure 4.12. The thermodynamic properties of all refrigerants were determined using the CoolPack V2.85 software. In the calculations of the refrigeration cycle, value of the evaporation temperature of the refrigerant was considered to be equal to the apparatus dew point temperature. Condensation temperature of the refrigerant was considered to be 15 °C above the atmospheric air temperature. In addition, superheated and subcooling temperature values were defined as 10 °C.

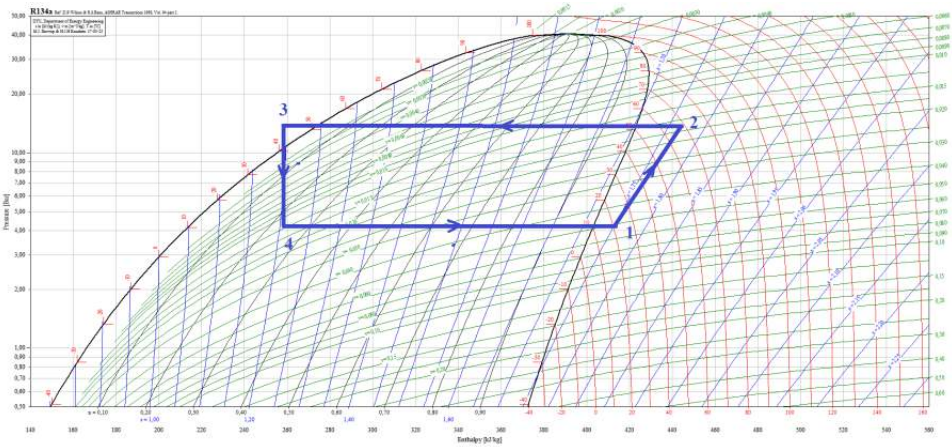

Figure 4.12. Pressure-enthalpy (P-h) diagram of the ICBAC system for the refrigerant R134a

Thermodynamic properties of the sample refrigerant R600a are given in Table 4.3. The obtained values for all refrigerants will be used for calculation of energy and exergy analysis of the ICBAC system in the following sections.

Table 4.3. Thermodynamic properties of the refrigerant R600a

Properties	Unit	Value
Condenser pressure, P_1	kPa	225.9
Condensation temperature, T_c	°C	51.8
Evaporator pressure, P_2	kPa	732.2
Evaporation temperature, T_e	°C	10.55
Compressor inlet temperature of refrigerant, T_1	°C	20.55
Compressor outlet temperature of refrigerant, T_2	°C	59.88
Condenser outlet temperature of refrigerant, T_3	°C	41.8
Evaporator inlet temperature of refrigerant, T_4	°C	10.55
Mass flow rate of refrigerant, $\dot{m}_{ref}$	°C	0.1707
Mass flow rate of air in condenser, $\dot{m}_a$	kg/s	6.1831
Mass flow rate of air in evaporator, $\dot{m}_s$	kg/s	2.233
Condenser inlet temperature of air, T_5	°C	36.8
Condenser outlet temperature of air, T_6	°C	46.08
Compressor isentropic efficiency, η	%	0.8446
Enthalpy at the point 1, h_1	kJ/kg	586.888
Enthalpy at the point 2, h_2	kJ/kg	642.911
Enthalpy at the point 3, h_3	kJ/kg	299.734
Enthalpy at the point 4, h_4	kJ/kg	299.734
Entropy at the point 1, s_1	kJ/kg.K	2.3639
Entropy at the point 2, s_2	kJ/kg.K	2.3920
Entropy at the point 3, s_3	kJ/kg.K	1.3360
Entropy at the point 4, s_4	kJ/kg.K	1.3530

Exergy analysis results of the ICBAC system for the sample refrigerant R134a is given in Table 4.4. In the analysis, the dead-state temperature (T_0) and the dead-state pressure (P_0) were considered to be environment temperature (36.8 °C) and 101.325 kPa, respectively. Moreover, the humid specific heat of moist air ($c_{p,air}$) was taken to be 1.0216 kJ/kg-dry-air.K in the calculation. Results of the ICBAC system for each refrigerant will be evaluated in the following sections.

Table 4. 4. Exergy analysis results of the ICBAC system for the refrigerant R134a

State No	Description	Fluid	Phase	Temperature (°C)	Pressure (kPa)	Enthalpy (kJ/kg)	Entropy (kJ/kgK)	Mass flow rate (kg/s)	Specific energy (kJ/kg)	Exergy rate (kW)
				T	P	h	s	$\dot{m}$	ex	$\dot{Ex}$
0	-	Air	Dead state	36.8	101.325	-	-	-	0	0
0	-	R134a	Dead state	36.8	101.325	434.73	1.934	-	0	0
1	Compressor inlet	R134a	Superheated vapor	20.55	4.222	412.893	1.750	0.3183	35.17	11.19
2	Compressor outlet	R134a	Superheated vapor	68.55	13.782	443.963	1.766	0.3183	61.28	19.51
3	Condenser outlet	R134a	Liquid	41.8	13.782	258.862	1.198	0.3183	52.15	16.60
4	Evaporator inlet	R134a	Mixture	10.55	4.222	258.862	1.208	0.3183	49.05	15.61
5	Condenser inlet	Air	Gas	36.8	101.325	-	-	6.1831	0	0
6	Condenser outlet	Air	Gas	46.13	101.325	-	-	6.1831	0.14	0.87
m	Evaporator inlet	Air	Gas	28.53	101.325	-	-	2.233	0.114	0.25
s	Evaporator outlet	Air	Gas	14.4	101.325	-	-	2.233	0.87	1.94

4.6. Energy and exergy analysis of the ICBAC system operating with different refrigerants

Figure 4.13 shows the effect of different refrigerants on COP values and the compressor input powers such as useful work and reversible power. As seen from this figure, R600a has the highest COP value and lowest useful work and reversible power for compressor. On the other hand, R404A has the lowest COP value and highest useful work and reversible power for compressor. Obtained COP values varied between 4.46 and 5.13 for studied refrigerants, resulting in up to 15% difference. Maximum useful work and maximum reversible power values are 10.99 kW and 9.37 kW, while minimum useful work and minimum reversible power values are 9.57 kW and 8.08 kW, respectively. The reversible power of 8.08 kW is the minimum power input that needs to be supplied to the compressor of the ICBAC system.

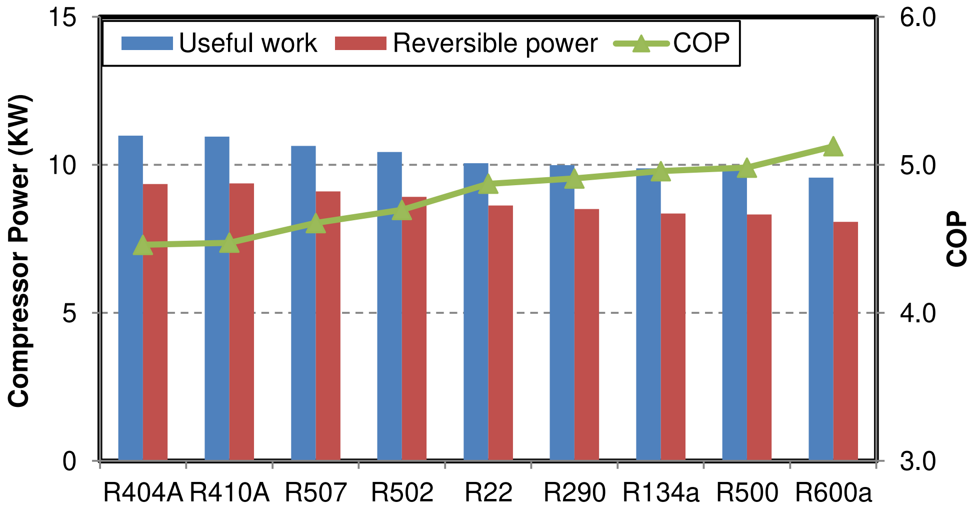

Figure 4.13. The effect of different refrigerants on COP values of the ICBAC system and compressor input powers such as useful work and reversible power

Figure 4.14 shows heat transfers in the condenser and evaporator for different refrigerants. As seen from this figure, R404A and R600a have the highest and lowest heat transfers in the condenser, respectively. By contrast, heat transfer in the evaporator (AC cooling capacity) has the same value, 49.03 kW, for all refrigerants. Maximum heat transfer in the condenser is 60.02 kW, and minimum heat transfer in the condenser is 58.60 kW, resulting in 2.44% difference. It is worth noting that determined value of the AC cooling capacity is very close to given value in the Figure 4.7 (48 kW), and this result validates the calculation performed.

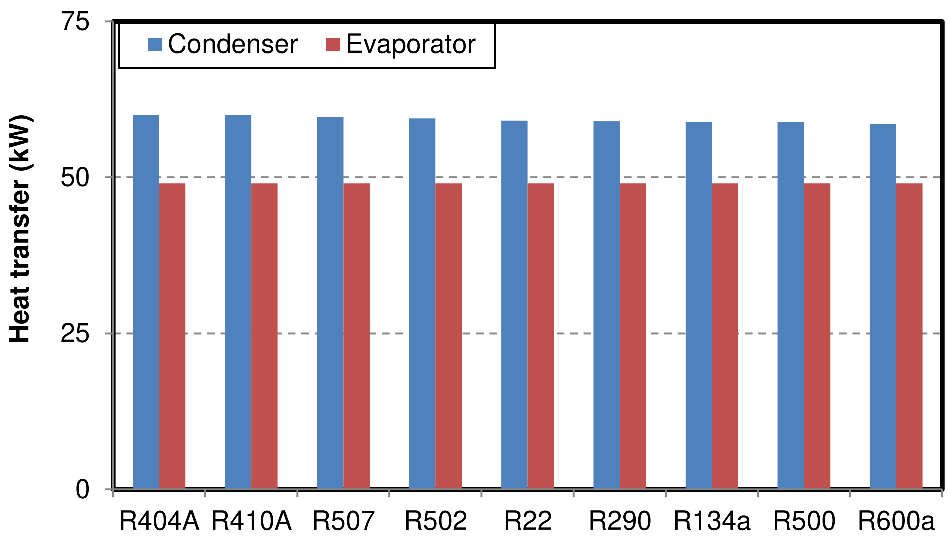

Figure 4.14. Heat transfers in the condenser and evaporator for different refrigerants

Figure 4.15 presents exergy destruction values of the ICBAC system equipment for different refrigerants. As shown in the figure, R410A has the highest exergy destruction values at evaporator and condenser, and R404A has the highest exergy destruction values at compressor and expansion valve. On the other hand, R600a has the lowest exergy destruction values at condenser and expansion valve.

R22 has the lowest exergy destruction value at compressor, and R500 has the lowest exergy destruction value at evaporator. Maximum exergy destruction values of evaporator, condenser, compressor and expansion valve are 2.83 kW, 2.57 kW, 1.64 kW and 1.82 kW, while minimum exergy destruction values of these components are 2.73 kW, 1.88 kW, 1.43 kW and 0.89 kW, respectively.

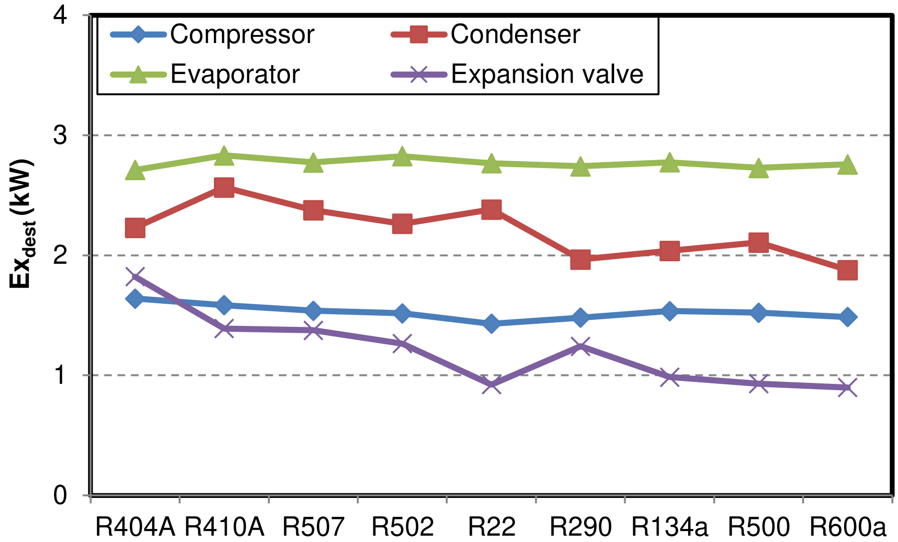

Figure 4.15. Exergy destruction values of the ICBAC system equipment for different refrigerants

Figure 4.16 displays exergy efficiency values of the ICBAC system equipment for different refrigerants. As shown in the figure, the exergy efficiency of each system equipment tends to vary slightly for different refrigerants. Expansion valve has the highest exergy efficiency values for all studied refrigerants, while condenser has the lowest values. Overall exergy efficiency and total exergy destruction values of the ICBAC system for different refrigerants are given in Figure 4.17. As can be observed from the figure, R600a has the highest overall exergy efficiency and lowest total exergy destruction, and R404A has the lowest overall exergy efficiency and highest total exergy destruction values.

Maximum overall exergy efficiency and total exergy destruction values are 46.45% and 8.40 kW, while minimum overall exergy efficiency and total exergy destruction values are 40.00% and 7.02 kW, respectively. It is worthwhile to mention that the refrigerant R134a, which is currently used in the TS 45 inter-city bus, has a lower overall exergy efficiency and higher total exergy destruction value than R600a.

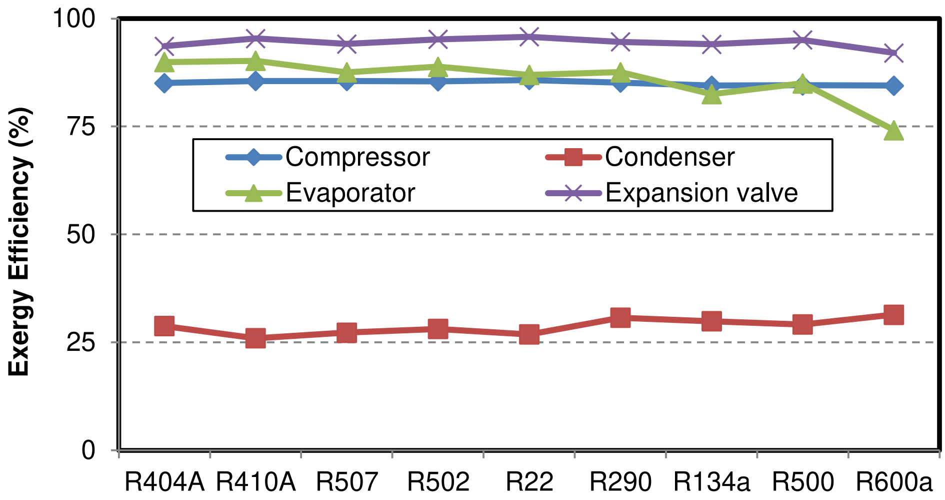

Figure 4.16. Exergy efficiency values of the ICBAC system equipment for different refrigerants

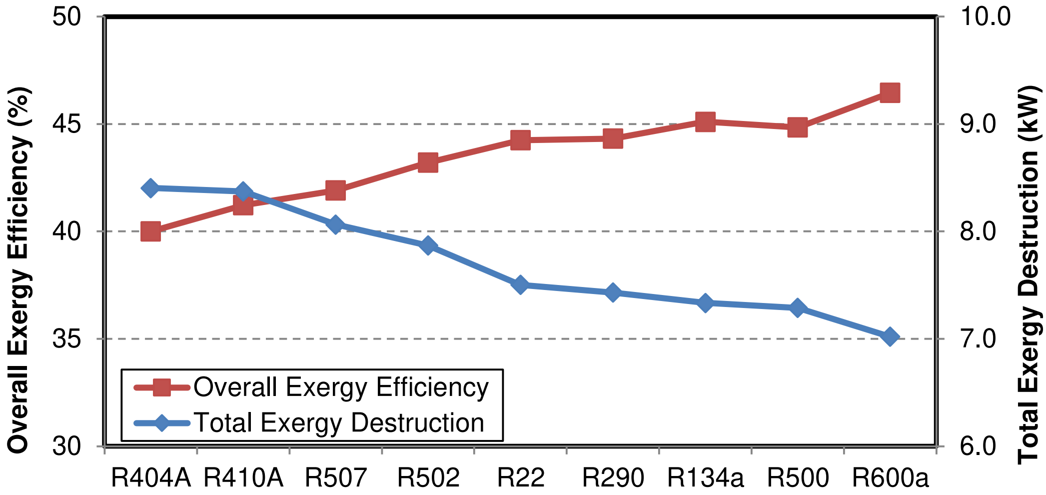

Figure 4.17. Overall exergy efficiency and total exergy destruction (kW) values of the ICBAC system for different refrigerants

4.7. Energy and exergy analysis of the ICBAC system for different air mixing ratios

Figure 4.18 displays the variation of heat transfer rates at evaporator with respect to MR for different refrigerants. As shown in the figure, heat transfer rates have the same values for all studied refrigerants. Maximum obtained heat transfer rate at the evaporator among all refrigerants is 49.030 kW for MR= 0.5, while minimum heat transfer rate is 30.75 kW for MR= 0.05. The most significant reason for heat transfer rate increment with increasing MR is the increment in the air mixture temperature and absolute humidity of outdoor air.

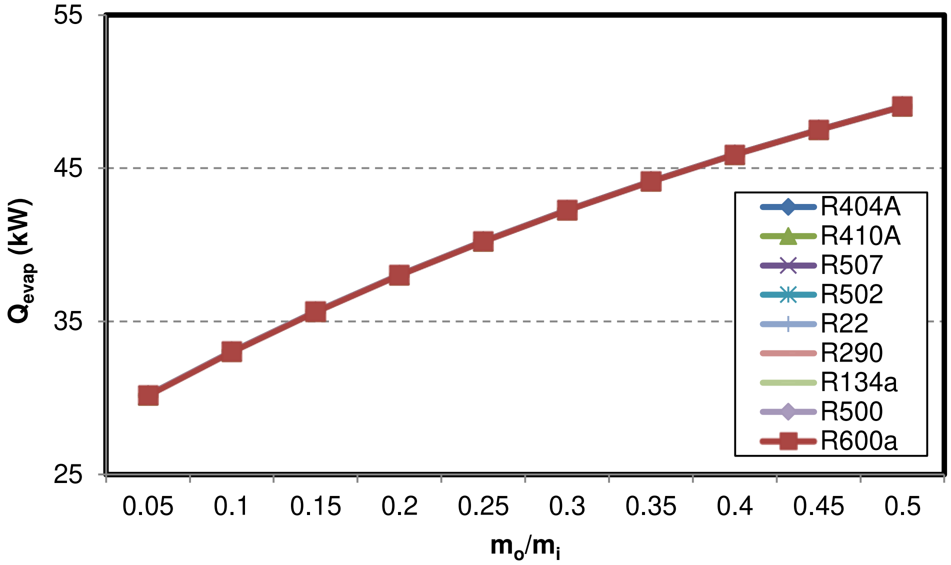

Figure 4.18. Variation of heat transfer rates at evaporator with respect to MR for different refrigerants

Figure 4.19 displays variation of heat transfer rates at condenser with respect to MR for different refrigerants. As shown in the figure, R600a and R404A have the highest and lowest heat transfer rates at condenser among all refrigerants, respectively. Maximum heat transfer rate is 60.02 kW and observed at MR= 0.5, while minimum heat transfer rate is 35.79 kW and observed at MR= 0.05.

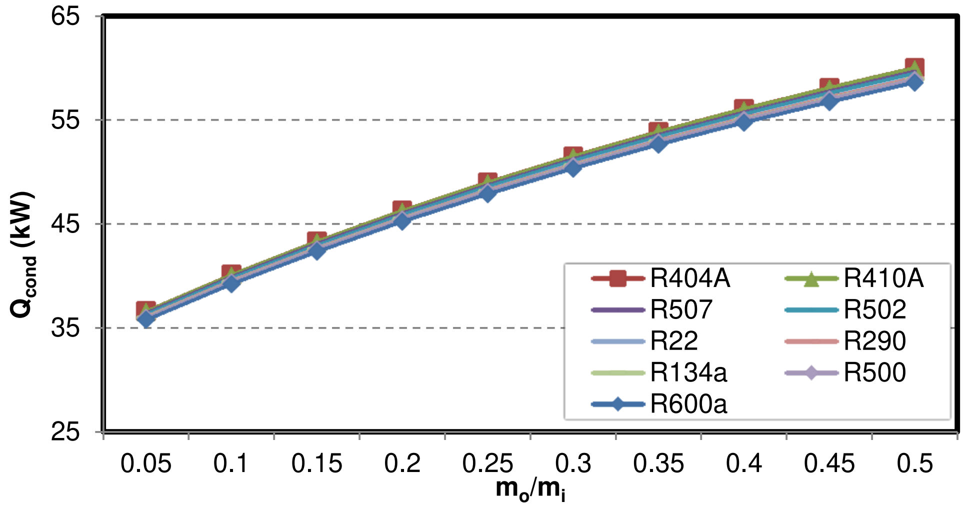

Figure 4.19. Variation of heat transfer rates at condenser with respect to MR for different refrigerants

Figure 4.20 displays the variation of compressor input powers with respect to MR for different refrigerants. As demonstrated in the figure, R600a and R404A have the lowest and highest compressor input powers among all refrigerants. Maximum compressor power is obtained as 10.99 kW at MR= 0.5, while minimum compressor power is obtained as 5.62 kW at MR= 0.05. It is important to note that the heat gain with lower outdoor air amount has lower value results in compressor power, and vice versa.

Figure 4.21 shows the variation of COP values of the ICBAC system with respect to MR for different refrigerants. As can be observed from the figure, R600a and R404A have the highest and lowest overall COP values among all refrigerants. Maximum COP value is 5.36 and observed at MR= 0.05, while minimum heat transfer rate is 4.46 and observed at MR= 0.5.

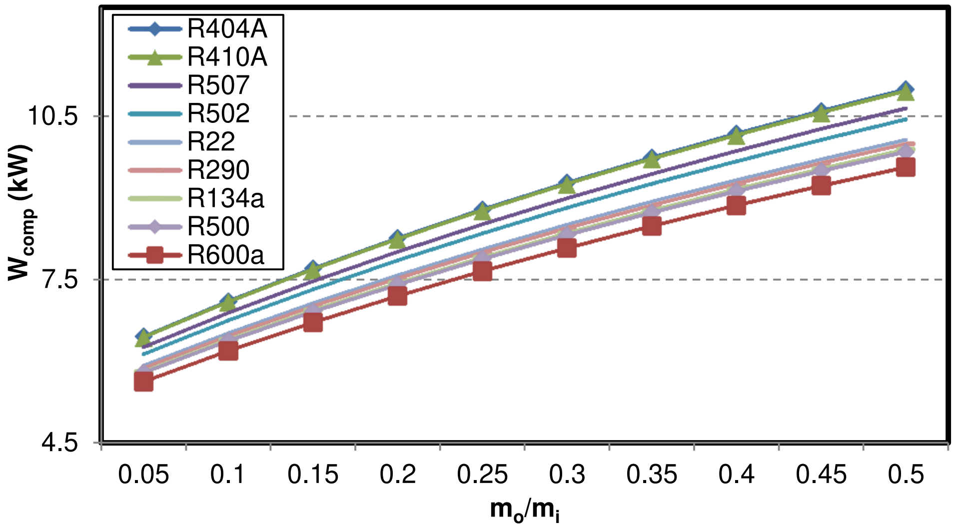

Figure 4.20. Variation of compressor input powers with respect to MR for different refrigerants

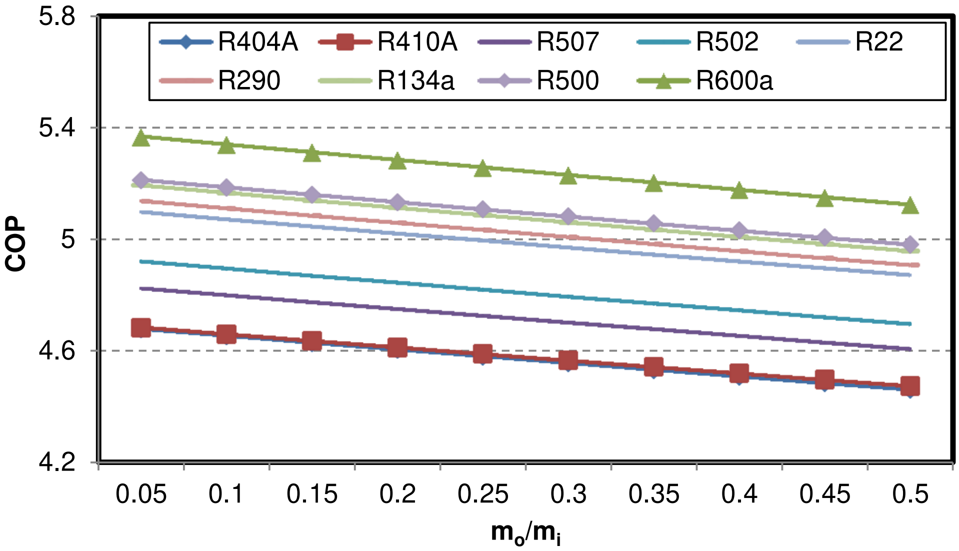

Figure 4.21. Variation of COP values of the ICBAC system with respect to MR for different refrigerants

According to the these figures, R600a has the most desirable overal result for the refrigeration system among studied refrigerants, while R404 has the least desirable overal result.

The effect of MR to exergy destruction values of ICBAC system components for different refrigerants are demonstrated in the Figures 4.22, 4.23, 4.24 and 4.25. It can be distinctly seen from the figures that exergy destruction values of each component increase with increasing MR for studied refrigerants. It can be concluded that air mixture temperature increment, which is a result of increasing ratio of outside air and absolute humidity of outdoor air, causes increasing in cooling load (heat gain) and exergy destruction values.

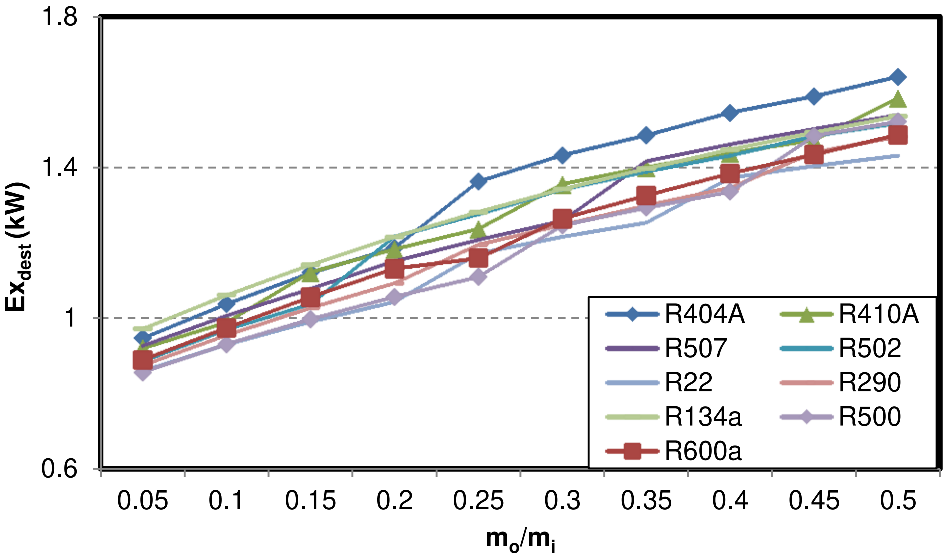

Figure 4.22. The effect of MR to exergy destruction values at compressor for different refrigerants

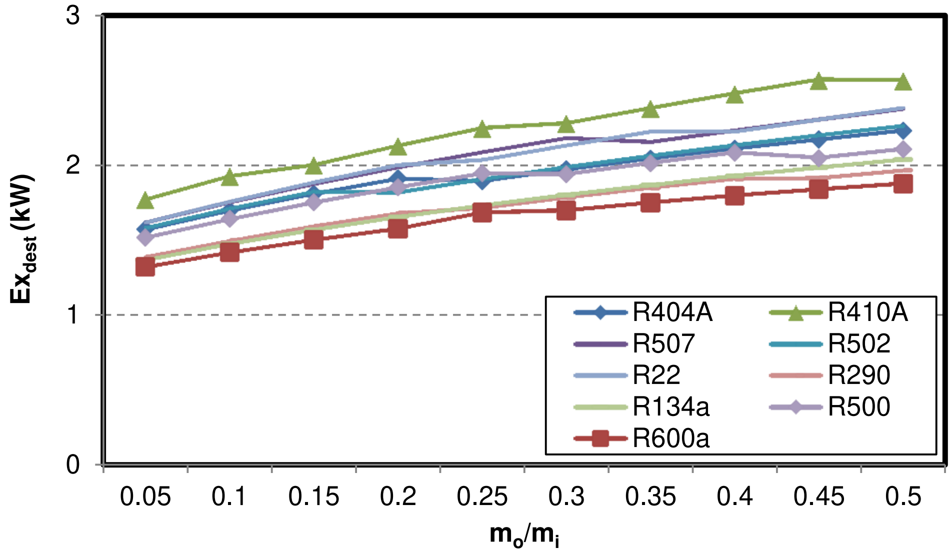

Figure 4.23. The effect of MR to exergy destruction values at condenser for different refrigerants

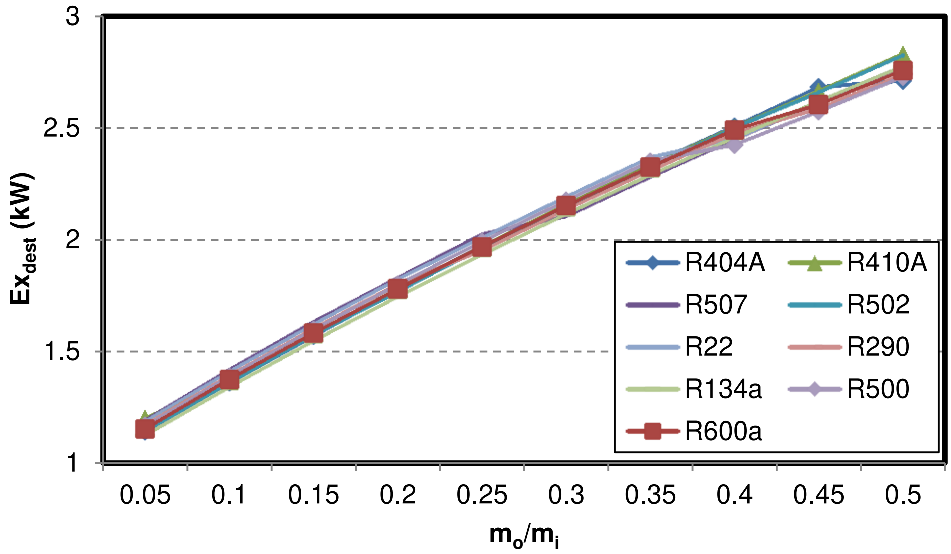

Figure 4.24. The effect of MR to exergy destruction values at evaporator for different refrigerants

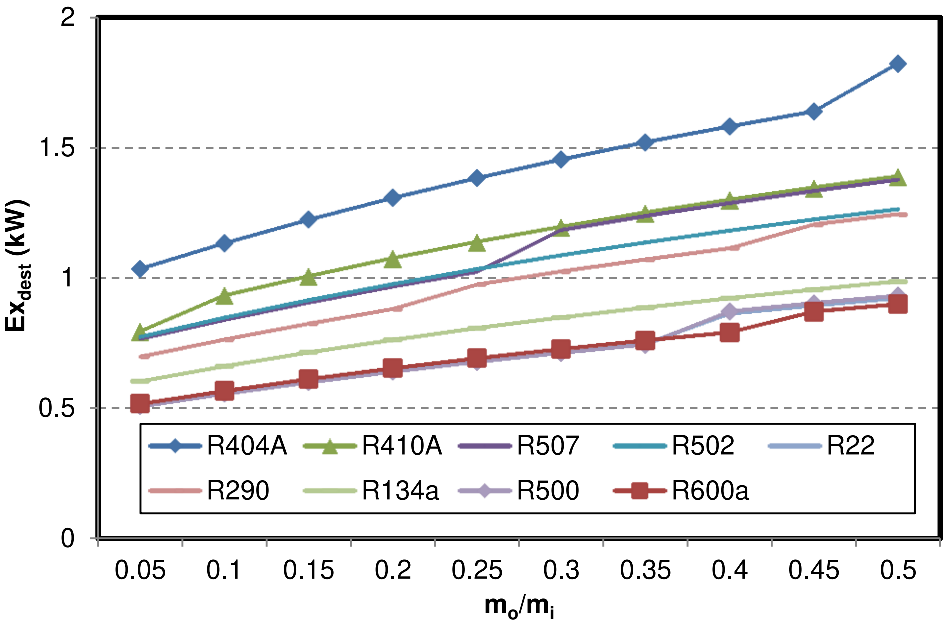

Figure 4.25. The effect of MR to exergy destruction values at expansion valve for different refrigerants

As previously mentioned, R600a has highest overall performance for the refrigeration system among all refrigerants, and R404A has lowest overall performance. Therefore, two refrigerants will be examined further.

Figure 4.26 shows effect of MR to exergy destruction values of the ICBAC system equipment for R600a and R404A refrigerants. As shown in the figure, exergy destructions of each equipment increase with increasing MR. Maximum exergy destruction is 2.71 kW and observed at evaporator (R600a). On the other hand, minimum exergy destruction is 0.51 kW and observed at evaporator (R600a). Exergy destruction values of R600a for evaporator, condenser, compressor and expansion valve at MR=0.5 are 2.75 kW, 1.87 kW, 1.486 kW and 0.89 kW, respectively. Additionally, exergy destruction values of R404A for evaporator, condenser, compressor and expansion valve at MR=0.5 are 2.711 kW, 2.23 kW, 1.643 kW and 1.82 kW, respectively.

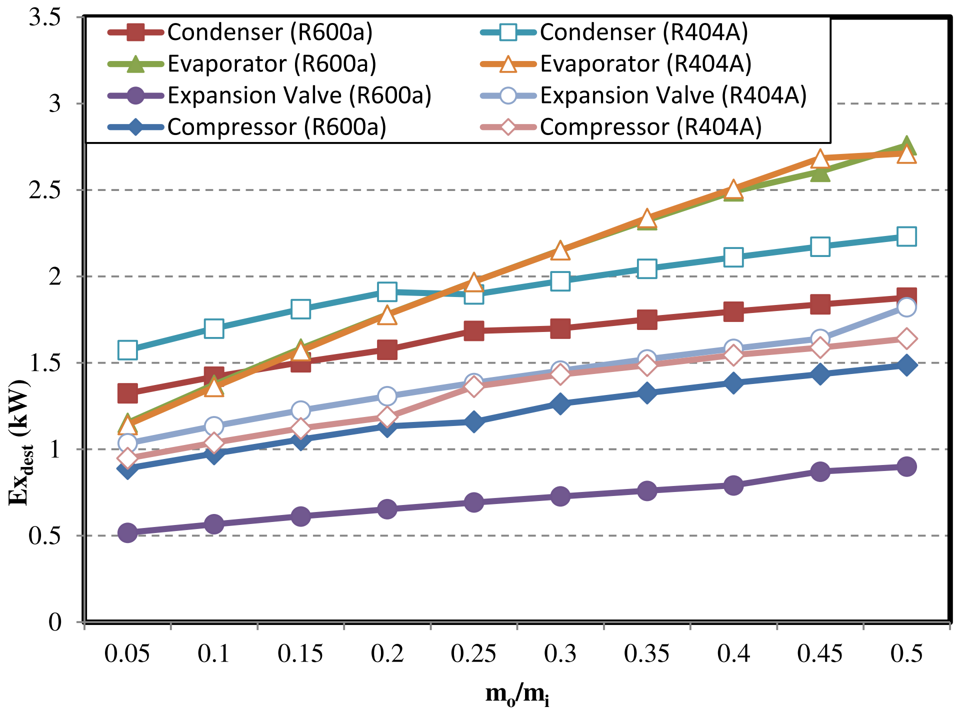

Figure 4.26. Effect of MR to exergy destruction values of the ICBAC system equipment for R600a and R404A

Effect of MR to exergy efficiency values of the ICBAC system equipment for R600a and R404A is shown in Figure 4.27. As presented in the figure, maximum exergy efficiency is 93.6% and obtained at expansion valve (R400a). On the other hand, minimum exergy efficiency is 28.8% and obtained at condenser (R400a). Exergy efficiency values of R404A for expansion valve, evaporator, condenser, compressor and condenser at MR=0.5 are 93.60%, 89.93%, 85.08% and 28.80%, while exergy efficiency values of R600a are 92.05%, 74.16%, 84.46% and 31.43%, respectively. It is important to note that exergy efficiency at condenser increases in parallel with MR values, while exergy efficiency at evaporator decreases. By contrast, exergy efficiencies at expansion valve and compressor are affected very slightly.

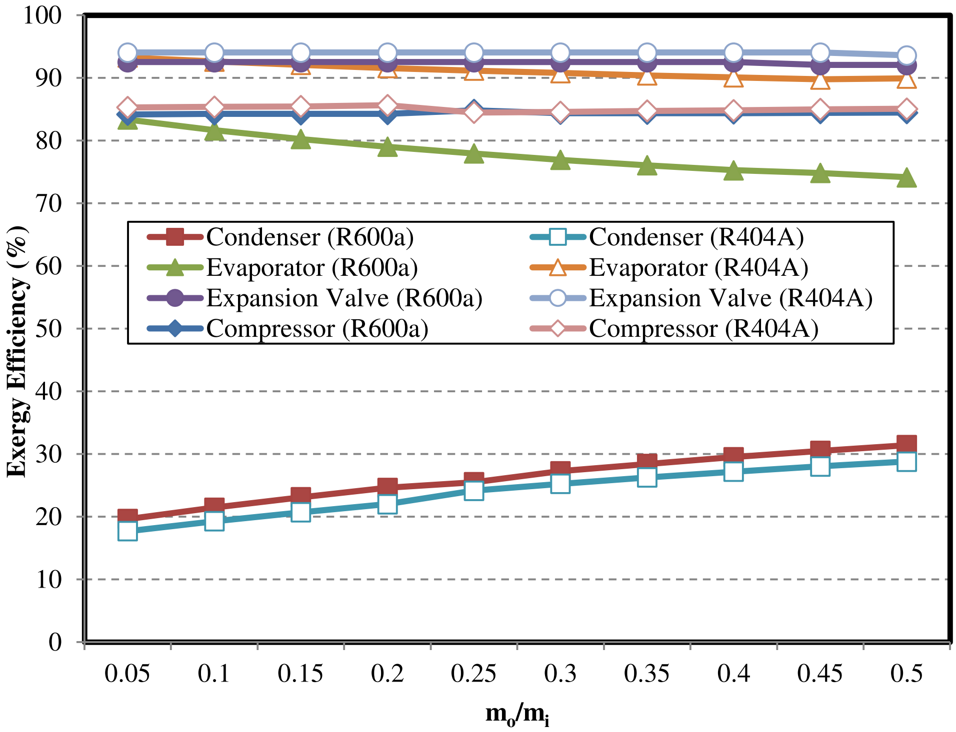

Figure 4.27. Effect of MR to exergy efficiency values of the ICBAC system equipment for R600a and R404A

Figure 4.28 presents effect of increasing MR to total exergy destruction values of the ICBAC system for different refrigerants. As demonstrated in the figure, R600a has the lowest total exergy destruction values, while R404A has the highest total exergy destruction values. Maximum total exergy destructions for R600a and R404A are 7.02 kW and 8.37 kW, while minimum total exergy destructions for R600a and R404A are 3.88 kW and 4.69 kW, respectively. It is worth noting that the refrigerant R134a, which is currently used in the TS 45 inter-city bus, has higher total exergy destruction values than R600a.

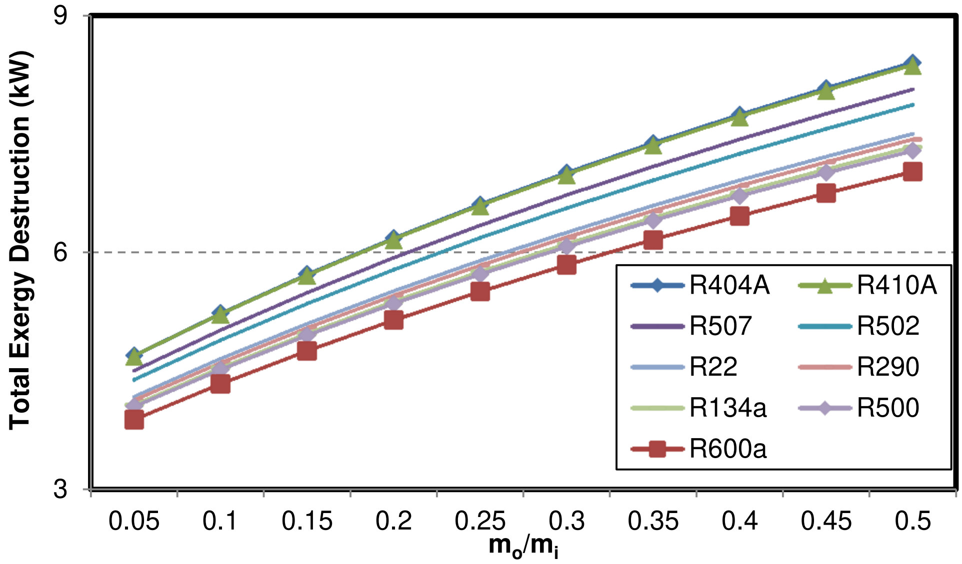

Figure 4.28. Effect of MR to total exergy destruction values of the ICBAC system for different refrigerants

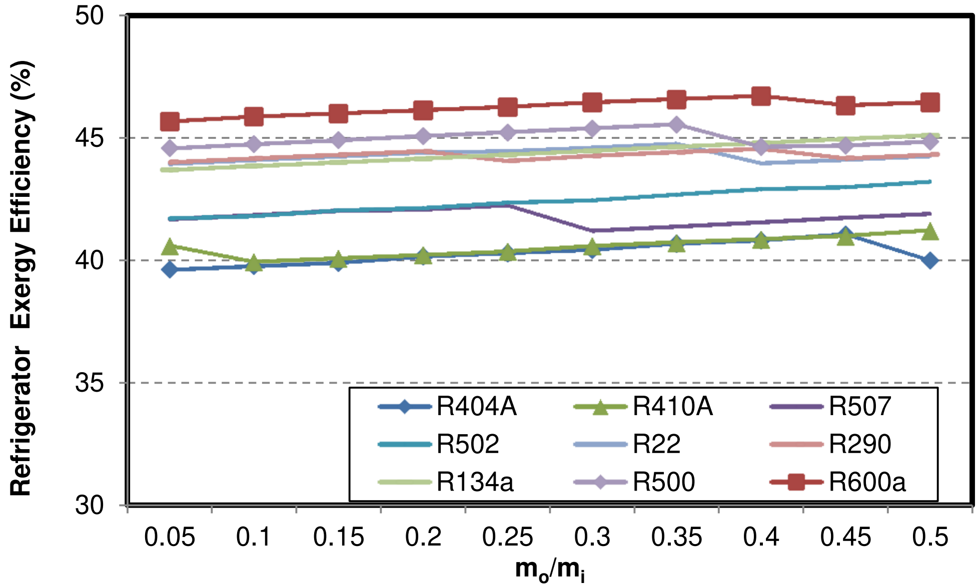

Figure 4.29. Effect of MR to overall exergy efficiency values of the ICBAC system for different refrigerants

Figure 4.29 shows effect of increasing MR to overall exergy efficiency values of the ICBAC system for different refrigerants. As presented in the figure, R600a has the highest exergy efficiency values, and R404A has the lowest exergy efficiency values. Exergy efficiency of the ICBAC system indistinctly increases in parallel with MR values. Maximum obtained exergy efficiencies for R600a and R404A are 46.45% and 40.00%, while minimum obtained exergy efficiencies for R600a and R404A are 45.67% and 39.62%, respectively. It is important to note that the refrigerant R134a, which is currently used in the TS 45 inter-city bus, has lower overall exergy efficiency values than R600a.

As can be observed from Figures 4.28 and 4.29, R600a has the highest exergy efficiency and lowest total exergy destruction. It can be concluded that R600a is the optimum refrigerant according to exergy analysis results. In this regard, R600a will be evaluated in a detailed way.

4.8. Energy and exergy analysis of the ICBAC system for the refrigerant R600a

The effect of MR on COP values of the ICBAC system and the compressor input powers such as useful work and reversible power for R600a is shown in Figure 4.30. Maximum useful work input and reversible power values are 9.57 kW and 8.08 kW, while minimum useful work input and reversible power are 5.62 kW and 4.73 kW, respectively. Determined COP values varied from 5.12 to 5.36 for the refrigerant R600a, resulting in up to 4.6% difference. It is observed that difference between useful work and reversible power increases significantly with increasing MR, thus resulting in reduction in COP.

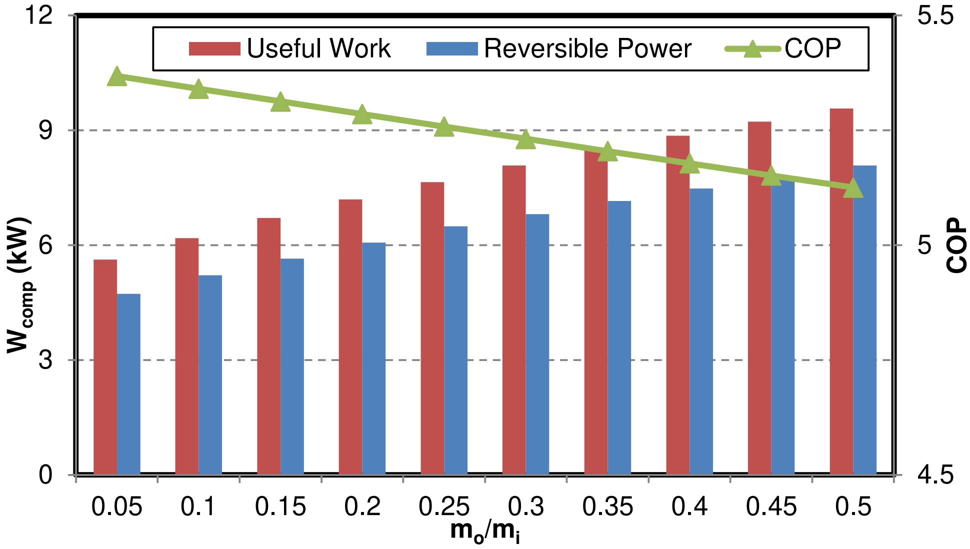

Figure 4.30. The effect of MR on COP values of the ICBAC system and the compressor input powers such as useful work and reversible power for R600a

Figure 4.31 shows the heat transfer rates at condenser and evaporator with respect to MR for R600a. As presented in the figure, minimum heat transfer at condenser is 35.79 kW and observed at MR=0.05, while maximum heat transfer value is 58.59 kW and observed at MR=0.5, causing 63.70% more energy consumption. On the other hand, minimum heat transfer at evaporator is 30.17 kW and obtained at MR=0.05, while maximum heat transfer at evaporator is 49.03 kW and obtained at MR=0.5, causing 62.51% more energy consumption. As stated previously, determined value of the AC cooling capacity at MR=0.5 is close to given value in the Figure 4.7 (48 kW). It is worthwhile to mention that increasing MR causes increment in the temperature and absolute humidity of air mixture. In this regard, it is the main reason for higher heat transfer rates.

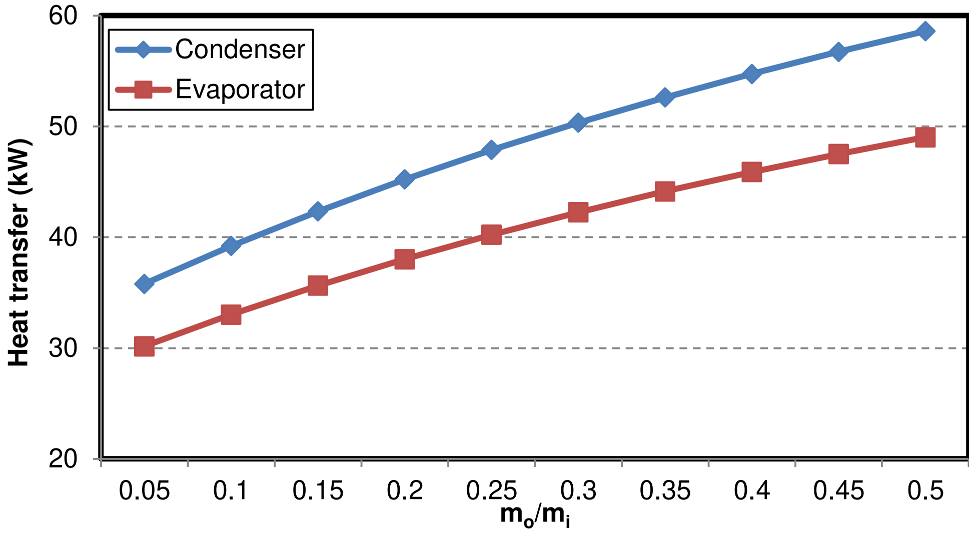

Figure 4.31. The heat transfer rates at condenser and evaporator with respect to MR for R600a

Figure 4.32 presents exergy destruction values of the ICBAC system equipment with respect to MR for R600a. As presented in the figure, exergy destruction values of each system equipment increases with increasing MR. Maximum exergy destruction values of evaporator, condenser, compressor and expansion valve are 2.75 kW, 1.87 kW, 1.48 kW and 0.89 kW, while minimum exergy destruction values of these components are 1.15 kW, 1.32 kW, 0.88 kW and 0.51 kW, respectively.

Figure 4.33 shows exergy efficiency values of the ICBAC system equipment with respect to MR for R600a. As demonstrated in the figure, exergy efficiency values of the each system component varies indistinctly with respect to MR. Exergy efficiencies of expansion valve, compressor, evaporator and condenser at MR=0.5 are 92.05%, 84.46%, 74.16% and 31.43%, whereas exergy efficiencies values at MR=0.05 are 92.52%, 84.18%, 83.36% and 19.64%, respectively. It is observed that expansion valve has the highest exergy efficiency values and condenser has the lowest exergy efficiency values for all MR values.

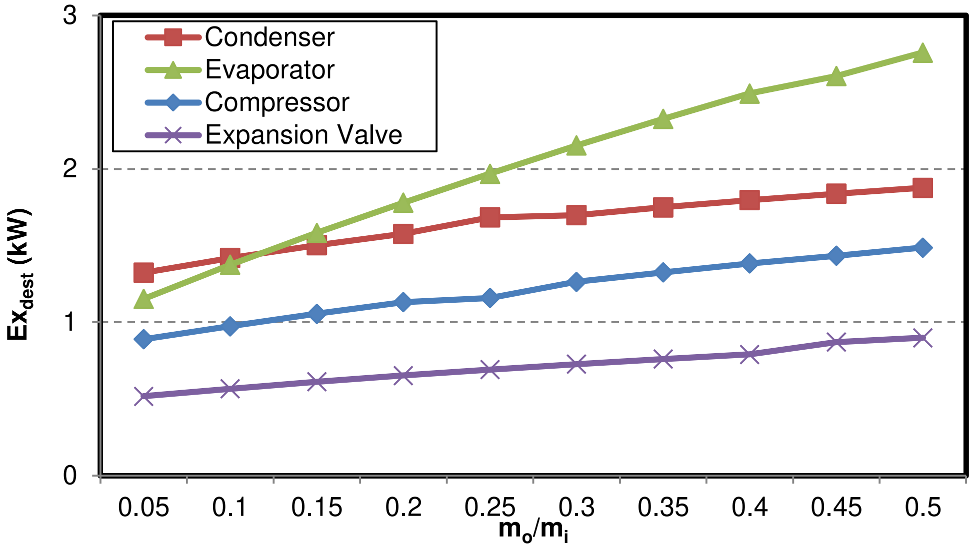

Figure 4.32. Exergy destruction values of the ICBAC system equipment with respect to MR for R600a

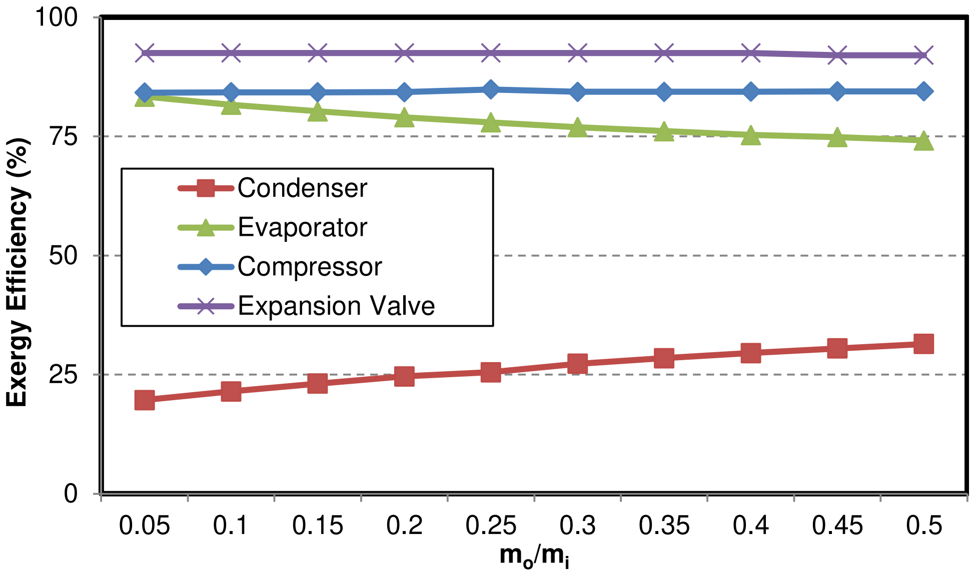

Figure 4.33. Exergy efficiency values of the ICBAC system equipment with respect to MR for R600a

Figure 4.34 displays the effects of overall exergy efficiency and total exergy destruction (kW) values of the ICBAC system with respect to MR for

R600a. As can be observed from the figure, total exergy destruction values increase significantly in parallel with MR values, while overall exergy efficiency values increase very slightly. Maximum overall exergy efficiency and total exergy destruction are 46.45% and 7.02 kW, and minimum overall exergy efficiency and total exergy destruction are 45.67% and 3.83 kW, respectively.

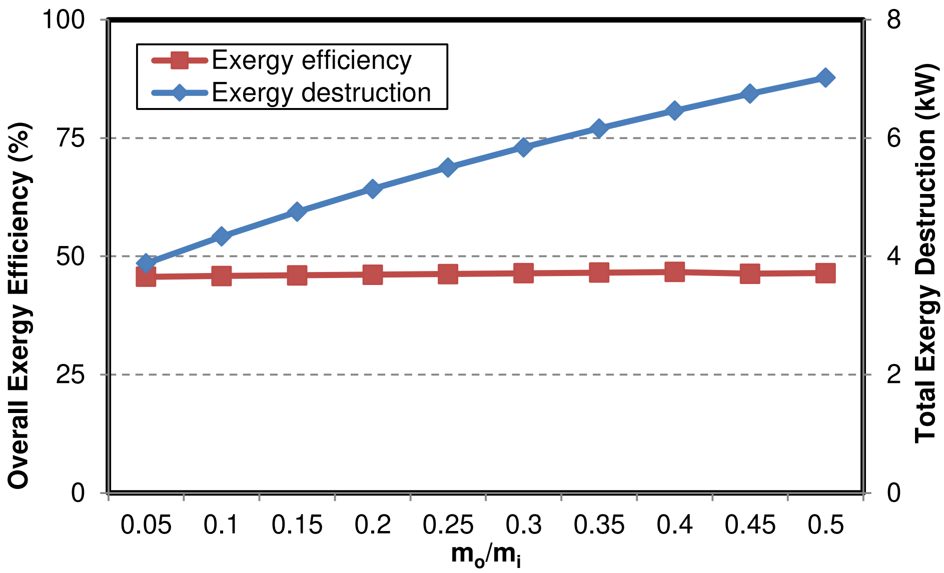

Figure 4.34. Overall exergy efficiency and total exergy destruction (kW) values of the ICBAC system with respect to MR for R600a

5. CONCLUSION

In this thesis, energy and exergy analysis are performed using different refrigerants and MRs to enhance the efficiency of the ICBAC system. It is important to note that higher system efficiency will lead to lower fuel consumption.

Adana province of Turkey was chosen as the study region. A coach bus, which is used for inter-city passenger transportation in United States, with a passenger capacity of 56 persons was selected. HAP was used to determine the hourly cooling load capacity of the selected inter-city bus. In the cooling load calculation of the inter-city bus, climate data such as dry bulb temperature, wet bulb temperature and solar radiation of the Adana province were used.

The load calculations and energy analysis were performed via ASHRAE-endorsed transfer function method and detailed 8760 hour-by-hour energy simulation techniques. Furthermore, typical refrigerants R404A, R410A, R502, R507, R22, R290, R134a, R500 and R600a were selected as different refrigerant types in the ICBAC system. The thermodynamic properties of selected refrigerants were computed using the CoolPack V2.85 program. COP, exergy efficiency and exergy destructions of the ICBAC system and its components are obtained and evaluated for all refrigerants.

In assumptions and analysis of the ICBAC system, MR value was considered to be between 0.05 and 0.5. Moreover, maximum value of heat gain is 25.96 kW and obtained at 17:00 in July. The inter-city bus cabin is maintained at 24.4 °C dry bulb temperature and 50% relative humidity, while the outside design conditions are 36.8 °C dry bulb temperature and 25.7 °C wet bulb temperature. It is worth noting that air mixture temperature increment, which is due to increasing ratio of outside air and absolute humidity of outdoor air, causes higher cooling load (heat gain) and exergy destruction values.

In calculations of the refrigeration cycle, the value of evaporation temperature of refrigerant was considered to be equal to the apparatus dew point temperature. Furthermore, outdoor air and indoor air were mixed at MR = 0.5, and the mixed air temperature was found to be 28.53 °C.

It is worth noting that the determined value (49.03 kW) of the AC cooling capacity was very close to given value in the Figure 4.7 (48 kW), and this result validated the calculation of ICBAC system and its components.

According to the obtained results, total exergy destruction values increase significantly in parallel with MR values, while overall exergy efficiency values increase indistinctly. Moreover, R600a has the highest overall exergy efficiency and lowest total exergy destruction among all studied refrigerants, while R404A has the lowest overall exergy efficiency and highest total exergy destruction. It is worthwhile to mention that the refrigerant R134a, which is currently used in the TS 45 inter-city bus, has a lower overall exergy efficiency and higher total exergy destruction value than R600a.

Maximum total exergy destructions for R600a and R404A were found as 7.02 kW and 8.37 kW, and they are obtained at MR=0.5. On the other hand, minimum total exergy destructions for R600a and R404A were found as 3.88 kW and 4.69 kW and they are obtained at MR=0.05. Maximum exergy efficiency for R600a is 46.45% and determined at MR=0.5, while maximum exergy efficiency for R404A is 40.00%. In addition, minimum exergy efficiencies for R600a and R404A are 45.67% and 39.62% and determined at MR=0.05. Results demonstrated that performance of the ICBAC system was substantially affected from refrigerants and MRs.

Study reveals that R600a is the optimum refrigerant for refrigeration system among all studied refrigerants. Minimum total exergy destruction value of R600a is obtained 3.88 kW for MR=0.05, and maximum total exergy destruction value is calculated as 7.02 kW for MR=0.5. The usage of R600a as a replacement of R134a in AAC systems should be investigated for further studies.

REFERENCES

Ali, S. M., and Chakraborty, A., 2015. Thermodynamic modelling and performance study of an engine waste heat driven adsorption cooling for automotive air-conditioning. Applied Thermal Engineering, 90(X), 54–63.

Alkan, A., and Hosoz, M., 2010a. Comparative performance of an automotive air conditioning system using fixed and variable capacity compressors. International Journal of Refrigeration, 33(3), 487–495.

Alkan, A., and Hosoz, M., 2010b. Experimental performance of an automobile air conditioning system using a variable capacity compressor for two different types of expansion devices. International Journal of Vehicle Design, 52, 160-176.

Aprea, C., Greco, A., and Maiorino, A., 2013. The substitution of R134a with R744: An exergetic analysis based on experimental data. International Journal of Refrigeration, 36(8), 2148–2159.

Bilgili, M., 2011. Hourly simulation and performance of solar electric-vapor compression refrigeration system. Solar Energy, 85(11), 2720–2731.

Bilgili, M., Ozbek, A., Yasar, A., Simsek, E., and Sahin, B., 2016. Effect of atmospheric temperature on exergy efficiency and destruction of a typical residential split air conditioning system. International Journal of Exergy, 20(1), 66–84.

Bobbo, S., Zilio, C., Scattolini, M., and Fedele, L., 2014. R1234yf as a substitute of R134a in automotive air conditioning. Solubility measurements in two commercial PAG oils. International Journal of Refrigeration, 40(0), 302–308.

Boles, M. A., and Cengel, Y. A., 2005. Thermodynamics An Engineering Approach. Journal of Cardiovascular Electrophysiology (5th ed.).

CARRIER., 2017. Hvac System Design Software. Retrieved April 1, 2017, from http://www.carrier.com/commercial/en/us/software/hvac-system-design/

CH Bus Sales., 2017. 2017-TS-45-Brochure. Retrieved April 1, 2017, from http://chbussales.com/new-coaches/ts-45

Chu, C.-M., and Jong, T.-L., 2008. Enthalpy estimation for thermal comfort and energy saving in air conditioning system. Energy Conversion and Management, 49(6), 1620–1628.

Datta, S. P., Das, P. K., and Mukhopadhyay, S., 2014. Obstructed airflow through the condenser of an automotive air conditioner - Effects on the condenser and the overall performance of the system. Applied Thermal Engineering, 70(1), 925–934.

Direk, M., and Hosoz, M., 2008. Energy and exergy analysis of an Automobile Heat Pump system. International Journal of Exergy, 5(5), 556-566.

Earth Policy Institute., 2014. Average Global Temperature, 1880-2013. Retrieved February 1, 2017, from http://www.earth-policy.org/data_center/C23

Gürtürk, M., and Oztop, H. F., 2016. Exergy analysis of a circulating fluidized bed boiler cogeneration power plant. Energy Conversion and Management, 120, 346–357.

Hosoz, M., and Direk, M., 2006. Performance evaluation of an integrated automotive air conditioning and heat pump system. Energy Conversion and Management, 47(5), 545–559.

Hürdoğan, E., Buyükalaca, O., Hepbasli, A., and Yılmaz, T., 2011. Exergetic modeling and experimental performance assessment of a novel desiccant cooling system. Energy and Buildings. 43(6), 1489-1498.

IEA., 2016. Contribution of technologies and sectors to global cumulative CO_2 reductions. Retrieved December 1, 2016, from https://www.iea.org

Kalaiselvam, S., and Saravanan, R., 2009. Exergy analysis of scroll compressors working with R22, R407c, and R417a as refrigerant for HVAC system. Thermal Science, 13(1), 175–184.

Kaushik, S. C., Reddy, V. S., and Tyagi, S. K., 2011. Energy and exergy analyses of thermal power plants: A review. Renewable and Sustainable Energy Reviews. Elsevier Ltd.

Khamis Mansour, M., Musa, M. N., Wan Hassan, M. N., and Saqr, K. M., 2008a. Development of novel control strategy for multiple circuit, roof top bus air conditioning system in hot humid countries. Energy Conversion and Management, 49(6), 1455–1468.

Khamis Mansour, M., Musa, M. N., Wan Hassan, M. N., and Saqr, K. M., 2008b. Thermoeconomic optimization for a finned-tube evaporator configuration of a roof-top bus air-conditioning system. Archives of Thermodynamics, 32(4), 290–305.

Li, G., Eisele, M., Lee, H., Hwang, Y., and Radermacher, R., 2014. Experimental investigation of energy and exergy performance of secondary loop automotive air-conditioning systems using low-GWP (global warming potential) refrigerants. Energy, 68, 819–831.

Ng, B. C., Darus, I. Z. M., Jamaluddin, H., and Kamar, H. M., 2014a. Application of adaptive neural predictive control for an automotive air conditioning system. Applied Thermal Engineering, 73(1), 1244–1254.

Ng, B. C., Darus, I. Z. M., Jamaluddin, H., and Kamar, H. M., 2014b. Dynamic modelling of an automotive variable speed air conditioning system using nonlinear autoregressive exogenous neural networks. Applied Thermal Engineering, 73(1), 1253–1267.

Ozbek, A., 2016a. Energy and exergy analysis of a ceiling-type air conditioning system operating with different refrigerants, 3, 36–54.

Ozbek, A, 2016b. Exergy characteristics of a ceiling-type residential air conditioning system operating under different climatic conditions. Journal of Mechanical Science and Technology, 30(11), 5247–5255.

Rana, A. H., and Mehta, J. R, 2013. Energy and Exergy Analysis of Extraction cum Back Pressure Steam Turbine. International Journal of ChemTech Research, 3(2), 626–632.

Schulze, C., Raabe, G., Tegethoff, W. J., and Koehler, J, 2014. Transient evaluation of a city bus air conditioning system with R-445A as drop-in - From the molecules to the system. International Journal of Thermal Sciences, 96, 355–361.

Sharafian, A., and Bahrami, M, 2014. Assessment of adsorber bed designs in waste-heat driven adsorption cooling systems for vehicle air conditioning and refrigeration. Renewable and Sustainable Energy Reviews, 30, 440–451.

Shek, K. W., and Chan, W. T, 2008. Combined comfort model of thermal comfort and air quality on buses in Hong Kong. Science of the Total Environment, 389(2–3), 277–282.

Solmaz, O., Ozgoren, M., and Aksoy, M. H, 2014. Hourly cooling load prediction of a vehicle in the southern region of Turkey by Artificial Neural Network. Energy Conversion and Management, 82, 177–187.

Suh, I. S., Lee, M., Kim, J., Oh, S. T., and Won, J. P, 2015. Design and experimental analysis of an efficient HVAC (heating, ventilation, air-conditioning) system on an electric bus with dynamic on-road wireless charging. Energy, 81, 262–273.

Sukri, M. F., Musa, M. N., Senawi, M. Y., and Nasution, H, 2015. Achieving a better energy-efficient automotive air-conditioning system: a review of potential technologies and strategies for vapor compression refrigeration cycle. Energy Efficiency, 8(6), 1201–1229.

Sun, X., Wu, J., and Wang, R, 2013. Exergy analysis and comparison of multi-functional heat pump and conventional heat pump systems. Energy Conversion and Management, 73, 51–56.

Temsa, 2016. TS45 - Training Document (Vol. 1). Adana: Temsa Ulaşım Araçları Sanayi ve Ticaret A.Ş.

Tobergte, D. R., and Curtis, S, 2013. Energy, Environment and Sustainable Development. Journal of Chemical Information and Modeling, 53(9), 1689–1699.

Tosun, E., Bilgili, M., Tuccar, G., and Aydın, K, 2016. Exergy analysis of an inter-city bus air-conditioning system, 20(4), 445-464.

TUIK, 2017. Motorlu Taşıt - Yıllara Bağlı Araç Sayısı. Retrieved March 1, 2017, from http://www.turkstat.gov.tr/Start.do

Tumen Ozdil, N. F., and Segmen, M. R, 2016. Investigation of the effect of the water phase in the evaporator inlet on economic performance for an Organic Rankine Cycle (ORC) based on industrial data. Applied Thermal Engineering, 100, 1042–1051.

Tumen Ozdil, N. F., Segmen, M. R., and Tantekin, A, 2015. Thermodynamic analysis of an Organic Rankine Cycle (ORC) based on industrial data. Applied Thermal Engineering, 91, 43–52.

Tumen Ozdil, N. F., Tantekin, A., and Erbay, Z, 2016. Energy and exergy analyses of a fluidized bed coal combustor steam plant in textile industry. Fuel, 183, 441–448.

Turkish Petroleum, 2015. Ham Petrol ve Doğalgaz Sektör Raporu.

Ünal, Ş, 2015. Determination of the ejector dimensions of a bus air-conditioning system using analytical and numerical methods. Applied Thermal Engineering, 90, 110–119.

Ünal, Ş., and Yilmaz, T, 2015. Thermodynamic analysis of the two-phase ejector air-conditioning system for buses. Applied Thermal Engineering, 79, 108–116.

Weilenmann, M. F., Alvarez, R., and Keller, M, 2010. Fuel Consumption and CO_2 Pollutant Emission of Mobile Air Conditioning at Fleet Level-New Data and Model Comparison. Environmental Science and Technology, 44(13), 5277–5282.

Yamaguchi, T., Tsuchiya, T., Nakahara, S., Fukui, A., Nagamoto, Y., Murotani, K., … Takahashi, N, 2016. Efficacy of Left Atrial Voltage-Based Catheter Ablation of Persistent Atrial Fibrillation. Journal of Cardiovascular Electrophysiology (5th ed., Vol. 27). New York.

Yilmaz, A, 2015. Transcritical organic Rankine vapor compression refrigeration system for intercity bus air-conditioning using engine exhaust heat. Energy, 82, 1047–1056.

Zhang, Q., and Canova, M, 2015a. Improving tracking performance of automotive air conditioning system via μ synthesis. Science and Technology for the Built Environment, 21(4), 448–461.

Zhang, Q., and Canova, M, 2015b. Modeling air conditioning system with storage evaporator for vehicle energy management. Applied Thermal Engineering, 87, 779–787.

CURRICULUM VITAE

Ediz ÇARDAK was born on February 17, 1990 in Adana. After graduated Adana Anatolia High School, he attended to Automotive Engineering Department of Çukurova University. He graduated from Çukurova University as an Automotive Engineer in 2013. He worked at Koluman Automotive Industry as a Production Engineer from July 2013 through March 2015. He's working at Temsa since January 2016. He's also studying for his Master's Degree at the Automotive Engineering Department of Çukurova University since 2013.